UNIVERSITY OF CALIFORNIA, SAN DIEGO

Chemically Programmable Immunity: Directing Pre-existing Antibodies to Attack and Clear Group A *Streptococcus* (GAS) Through Alphamer-mediated Therapy

A Thesis submitted in partial satisfaction of the requirements for the degree

Master of Science

in

Biology

by

Hojoon Kyujin Hwang

Committee in charge:

Victor Nizet, Chair
Ethan Bier, Co-Chair
Raffi Aroian
Sascha Kristian
Joseph Pogliano
George Sakoulas

2013

The Thesis of Hojoon Kyujin Hwang is approved, and it is acceptable in quality and form for publication on microfilm and electronically:

Co-Chair

Chair

University of California, San Diego

2013

DEDICATION

To my fellow Nizetians, friends, and family

Thank you! If I were to sum up my experience as a Master's student, it would be a giant "thank you" to everyone who has helped me along the way. I was blessed to be in the guidance of many friends and mentors in the Nizet lab, starting all the way from Samira Dahesh in 2011 to Dr. David Gonzalez and Dr. George Sakoulas in 2012, and most importantly, Dr. Sascha Kristian, without whom this thesis would not have been possible. I was a young (still young, I think), shy teenager who walked into a daunting place called "lab" and found himself bombarded by scientific jargons and papers that he was supposed to know about. It surprises me that the person who most helped me adjust to this new environment was the big boss himself, Professor Victor Nizet, who became my guide in the world of science.

Samira – I still think of you as my boss and your bacterial streaks look like a piece of modern art (in a good way!). Thank you for your heart-filling presence in the lab. David – your projects are cool and awesome! And it must be thrilling to know that you may be "Professor" Gonzalez soon! George – clinical rounds at Sharps Memorial Hospital were informative and memorable (especially with all the "zebra" cases we saw); equally significant were the talks we had to and from Sharps. You gave me valuable insights (economy and politics) and advices (traveling to Europe!) as a mentor.

Sascha – the first impression I have of you is very "interesting." Something about your height and buff arms... Anyways, it was very difficult to work at such a high pace at times (Wdee Thienphrapa would motion "whipping" whenever she saw me working late in the lab), but wow, how I miss having so much work. Sincerely, your dedication for your work is something that I truly admire and will look back to whenever I'm feeling unmotivated. You were also very good at making sure that I understood each and every aspect of the project (you even quizzed me to make sure!), and I eventually made that my style of teaching. You've taught me how to efficiently work (there were a couple of serious talks in Dr. Mary Hensler's side of the office), write "Sascha-quality" protocols (Dr. Laura Crotty Alexander likes them!), think critically on my own (complement deposition "report" essay comes to my mind), and everything that is in this thesis. More than a hundred experiments were conducted in just a year and I really am grateful for your help and guidance. Thank you.

Last but not least, Victor – thank you for your trust in me. When I started in your lab, I was an overly ambitious pre-medical student with a ridiculous plan to graduate in two years (still surprised I got through that). The primary purpose for joining your lab was to fulfill that "annoying" requirement for medical schools while buffing up my resume with a Master's degree. I knew nothing else except that I wanted to help those afflicted with diseases of poverty, and thought studying bacterial pathogenesis would be the most relevant research experience. Little did I know that I would come to like the lab and the experiments, and the two years I've been under your care have convinced me to pursue a MD/PhD degree instead. The first meeting I've had with you alone was probably the most nerve-wrecking experience aside from

the thesis defense. In the usual meetings with you and Sascha, I was nervous already presenting the past week's experiment results to you, but talking to the big boss by myself was on a whole different level of anxiety. I am glad that, however, after the first couple meetings, I was a bit more comfortable talking about my career plans and personal goals (as well as Psy's Gangnam Style!). In those meetings, you told me how your lab operates – how you orchestrate all the players in a dynamic research field, what you expect out of me, what others probably expect out of me (which was very helpful), and, among other things, your invaluable experiences as both a physician and a scientist. You always pointed me to the right direction and trusted me to carry on. Thank you for believing in me with a giant collaborative project that became this thesis. Thank you for your guidance and trust, Victor.

To my roommates since Stewart Hall – Andrew Kau, Kenji Oberlander, Matthew Hu, and Jeffrey Xu – thank you always for your company and support. Three years went by kind of fast, but with many memories!

To my dearest family – my brother Kyusuk, my mother Kyungsook, and my father Soonha Hwang – thank you for your love and care. You were always with me and for me, even when I pushed you away. Thank you.

EPIGRAPH

"Blessed is he who expects nothing, for he shall never be disappointed."

Jonathan Swift

TABLE OF CONTENTS

LIST OF FIGURES

LIST OF TABLES

ABSTRACT OF THE THESIS

Chemically Programmable Immunity: Directing Pre-existing Antibodies to Attack and Clear Group A *Streptococcus* (GAS) Through Alphamer-mediated Therapy

by

Hojoon Kyujin Hwang

Master of Science in Biology

University of California, San Diego, 2013

Professor Victor Nizet, Chair

Antibiotic-resistant bacteria such as methicillin-resistant *Staphylococcus aureus* (MRSA) and multi-drug resistant *Pseudomonas aeruginosa* present a growing concern for global health and safety. Because infections caused by such pathogens are often difficult to treat with standard antibiotics, the development of novel therapies is urgently needed. We are proposing an entirely novel approach to anti-infective therapy mediated by aptamers, an emerging therapeutics class, conjugated with the "alpha-Gal" epitope of galactosyl-alpha-l,3-galactosyl-beta-l,4-N-acetylglucosamine. The

conjugated aptamer, or “alphamer,” could theoretically immunize the host and lead to bacterial clearance through complement activation and phagocytosis by redirecting preexisting antibodies against the target pathogen.

The main goal of the thesis project, conducted in collaboration with Altermune Technologies, LLC, was to establish proof-of-concept (POC) for the proposed alphamer-mediated therapy utilizing a published group A *Streptococcus* (GAS) specific DNA aptamer, 20A24P. Firstly, the binding of 20A24P to multiple GAS serotypes was confirmed. Truncating 20A24P enhanced the binding affinity to GAS, and the target antigen of 20A24P was determined to be the M1 protein. A 5’-alpha-Gal alphamer conjugate of 20A24P, named α20A24P, was synthesized and binding to GAS strains observed. In addition, α20A24P was capable of recruiting mouse IgG and IgM antibodies, promoting phagocytosis of GAS by purified human neutrophils and inhibiting the outgrowth of a hypervirulent GAS strain in human blood. To further determine the potential of alphamers as novel anti-bacterial drugs, ongoing experiments explore the activity of α20A24P in GAS killing assays with phagocytes and in a mouse model of necrotizing fasciitis that were established in this project.

INTRODUCTION

Overview of the current state

Infections caused by drug-resistant bacteria are difficult to treat and exert a staggering toll on the public health worldwide. For example, in the United States, *Staphylococcus aureus* alone colonizes approximately 30% of healthy humans' nasopharynges or on their skin (1). Methicillin-resistant *S. aureus* (MRSA) kills 18,000 Americans every year, more than HIV/AIDS, Parkinson's disease, and homicide combined (2, 3). In hospital settings, infections caused by antibiotic resistant bacteria often complicate medical procedures such as surgery. Two million Americans develop these hospital-acquired infections (HAIs) per year, resulting in nearly 100,000 deaths, 20,000 of which are a direct result of antibiotic-resistant infections (4, 5). Outside of hospital settings, infections can spread in communities and these community-acquired infections (CAIs) such as pneumonias pose serious medical challenges as well. Compounding these infections are bacterial resistances to antibiotics. *Streptococcus pneumoniae* is the leading cause of community-acquired pneumonia (CAP), and approximately 30% of *S. pneumoniae* isolates in the United States are considered multidrug-resistant (6). The annual burden of antibiotic-resistant infections on U.S. health care system is as high as $20 billion in excess health care costs and more than 8 million additional hospital days (5).

Statement of the problem

Despite these overwhelming healthcare concerns with antibiotic resistant infections, the development of drugs to combat these bacterial pathogens has been waning. One early antibiotic drug to combat infectious diseases was discovered in 1928 by Dr. Alexander Fleming. His discovery of penicillin revolutionized the field of medicine and since then, there has been a continuous effort to discover more drugs with antimicrobial properties. However, the discoveries of such drugs have dwindled down to the current state: whereas 30 novel antibacterial agents were discovered between 1983 and 1992, only 7 additional agents were discovered in the last ten years (2, 7). While the antibiotic development pipeline is "running dry," the antibiotic resistance in bacteria is skyrocketing and the percentage of bacteria isolated with antibiotic resistance is constantly on the rise; therefore the development of novel anti-bacterial therapies is urgently needed.

Alphamer-mediated therapy

One novel approach to address the growing challenge of antibiotic resistance bacteria is the "Altermune" method, a patented concept of Dr. Kary Banks Mullis. Specifically, the technology can theoretically be applied to chemically program one's immune system and combat bacterial infections by redirecting preexisting high-titer antibodies in humans to bacterial pathogens creating immediate antibody-mediated immunity. Immediate immunity against a target pathogen is accomplished by an "alphamer," which is a DNA, RNA, or modified nucleic acid aptamer conjugated with the alpha-galactosyl ("alpha-Gal") epitope of galactosyl-alpha-l,3-galactosyl-beta-l,4-N-acetylglucosamine.

The alpha-Gal epitope is a carbohydrate expressed on glycoconjugates in many mammals, but not in Old World monkeys, apes, and humans. (8) Anti-alpha-Gal immunoglobulin G (IgG) is the most abundant natural antibody in humans, constituting approximately 1-3% of immunoglobulins with 1% of all B lymphocytes producing the anti-alpha-Gal. (9, 10) Recognition of the alpha-Gal epitope by preexisting anti-alpha-Gal IgG antibodies opsonizes the carbohydrate-containing molecule for complement activation, deposition of complement component C3b, and phagocyte engulfment through complement receptors and phagocytosis mediated by Fc receptors.

Alphamer: aptamer conjugated with the alpha-Gal epitope

Aptamers are single-stranded oligonucleotides that bind to target whole-cells or ligands with high affinity and specificity comparable to those of antibodies. Aptamers are selected from libraries of random oligonucleotides through an iterative *in vitro* selection-amplification process known as systematic evolution of ligands by exponential enrichment (SELEX; 11) In addition to their binding capabilities, aptamers' readily scalable production, non-immunogenicity, smaller size, thermal stability, potential to be nuclease-resistant, and ease of modification and conjugation all offer advantages of their use as therapeutic molecules over antibodies (12).

An alphamer – an aptamer that binds specifically to the target pathogenic bacterium or its ligand (e.g. lipopolysaccharides [LPS] of *Escherichia coli* [*E. coli*]) conjugated with the alpha-Gal epitope – can theoretically immunize the host against

the target and direct preexisting antibodies in the human host to attack and clear the pathogen (**Fig. 1**).

Proof-of-concept (POC) for the alphamer-mediated therapy

In this thesis, we tested for anti-bacterial efficacy of alphamers with the model bacteria with *Streptococcus pyogenes,* also known as group A *Streptococcus* (GAS). GAS is a Gram-positive, β-hemolytic bacterial pathogen. GAS infections can cause mild to life-threatening diseases, from streptococcal pharyngitis and impetigo to necrotizing fasciitis and streptococcal toxic shock syndrome. The global burden of invasive GAS disease is high, with over 150,000 deaths and 650,000 new cases each year (5).

The aptamer used for the POC study originated from a study by Hamula and colleagues, where 9 DNA aptamers were described to bind to multiple serotypes of GAS (13). In particular, aptamers 20A24P and 15A3P were determined to be the most promising, displaying high affinity and selectivity for a mixture of 10 different GAS serotype strains and estimated dissociation constants (K_d) of 9 nM and 10 nM, respectively (13).

To establish POC for the proposed alphamer-mediated therapy, a lead candidate aptamer was first prioritized. Then, the aptamer's binding capacity was characterized, and after determining the target antigen of the lead aptamer, the alpha-Gal epitope was conjugated to generate the alphamer. Binding patterns of the alphamer was confirmed to be identical to those of the aptamer, and we observed that the alphamer was able to redirect IgG and IgM antibodies to its target. Next,

opsonophagocytosis assay (OPA) showed that the alphamer promotes the uptake of target bacteria by purified human neutrophils (hPMNs), and other functional activity assay models were established. Lastly, an *in vivo* mouse model was established where future experiments can further illustrate the anti-bacterial capacity of alphamers and the potential of alphamers as a novel anti-bacterial drugs.

MATERIALS AND METHODS

Bacterial strains and culture conditions

Group A *Streptococcus* (GAS) strains used for this thesis were the GAS M1 wild-type strain (serotype M1T1; 14) 5448 an isogenic M1 protein-deficient GAS M1T1 5448 Δ*emm1* strain (15), an isogenic GAS M1T1 5448 Δ*emm1* mutant strain complemented with *emm1* gene *in trans* with plasmid pDCerm-*emm1* (15), an isogenic capsule-deficient GAS M1T1 5448 Δ*hasA* (16), GAS M1T1 5448 Δ*sdaI* (17), GAS M1T1 5448 Δ*speB* (18), GAS M1T1 animal-passaged (AP; 16), GAS M1 SF370 (ATCC 700294), GAS M3 20224 (from Dr. Malak Kotb's lab; University of North Dakota School of Medicine and Health Sciences, Grand Forks, ND), GAS M4 (CDC 4063-05 from the Centers for Disease Control and Prevention (CDC), Atlanta, GA), GAS M11 NS414 (19), GAS M12 NS488 (19), GAS NZ131 (M49T14; ATCC BAA-1633) and GAS M77 NS236 (19).

All strains were stored frozen as glycerol stocks at -80°C. For daily use, bacteria from glycerol stocks were streaked out on Todd-Hewitt agar (THA; Difco Laboratories) plates, grown overnight, and then stored at 4°C. Todd-Hewitt Broth (THB) cultures were inoculated from a streak of colonies from the THA plates and incubated overnight without shaking. Appropriate antibiotics were used for mutant strains at the following concentrations: 2 μg/mL chloramphenicol and/or 2 μg/ mL erythromycin. All incubations were done in normal atmosphere incubators at 37°C.

The growth phase of all THB cultures were assessed by measuring the optical density at 600 nm (OD_{600}) with a GENESYS 10UV-Vis Spectrophotometer (Thermo

Fisher Scientific, Inc.), where bacteria were expected to reach OD_{600} of 0.8 or 0.9, which correlate to late exponential or stationary growth phase after overnight incubation. At the start of most assays, 1 μL of broth culture was streaked out on a THA plate and incubated overnight at 37°C. After incubation, bacterial colonies were checked for their morphology. GAS colonies were expected to be white and non-translucent. Catalase test was done by placing a drop of 30% hydrogen peroxide solution (Thermo Fisher Scientific, Inc.) on to some colonies. GAS cells are catalase negative and cannot catalyze the decomposition of H_2O_2 to O_2 and H_2O; thus bubble formation would indicate a contamination with a catalase enzyme positive organism. Bacteria were determined to be GAS if they looked uniformly like GAS – cocci in pairs and chains – and were catalase enzyme negative, as indicated by absence of oxygen bubbles when bacterial cells were mixed with hydrogen peroxide.

DNA aptamers and alphamers

Nine published DNA aptamers with high affinity for GAS (13), truncated variant GAS aptamers, and a number of negative control aptamers, were used in this thesis. The nine published GAS aptamers were: 20A1P, 20A8, 20A8P, 20A9, 20A9P, 20A12P, 20A14P, 20A24P, and 15A3P. The truncated variants were: 20A24P.A2, 20A24P.A3, 20A24P.A4, 20A24P.A5, 20A24P.A6, 20A24P.A8, and 20A24P.A9. The negative control aptamers used for this study were: RAND-39, RAND-52, and RAND-80. The secondary structures of all tested aptamers, predicted by lowest free energy using the Mfold web server for nucleic acid folding and hybridization prediction (20), are shown in **Figure 2**.

The following oligonucleotide modifications were incorporated into aptamers: 3'- or 5'-6-Carboxyfluorescein (FAM; green fluorescent dye), 5'-TYE 665 (red fluorescent dye), 3'-Biotin-TEG (linker), 5'-alpha-gal epitope (trisaccharide antigen Galα1-3Galβ1-4GlcNAc), 3'-inverted dT (modified nitrogenous deoxythymidine base). All aptamers except alphamers were synthesized by Integrated DNA Technologies (Coralville, IA) and alphamers were synthesized by Biosearch Technologies (Novato, CA). Sequences of the aptamers and the alphamers with their modifications are listed in **Table 1**.

Before every experiment, the respective aptamers in H_2O or DPBS were pre-heated for 15 min at 72-80°C and then cooled to room temperature to allow for re-folding.

Flow cytometry: aptamer and alphamer binding

Bindings of aptamers and alphamers were assessed with a FACSCalibur flow cytometer (Becton, Dickinson and Company, Inc.) with CellQuest software (Becton, Dickinson and Company, Inc.) and data were analyzed with FlowJo (Tree Star Inc.) software. In general, flow cytometer samples were prepared in duplicates as follows: GAS cells cultured in THB were washed twice with Dulbecco's Phosphate Buffered Saline without calcium and magnesium (DPBS; Life Technologies, Inc.); centrifugation steps were carried out at 10,000 x *g* for 3 minutes, and then resuspended in equal volume of DPBS. OD_{600} of the washed culture was measured 1:10 diluted in DPBS in a polystyrene cuvette (Thermo Fisher Scientific, Inc.) with a spectrophotometer, with DPBS as the blank.

Bacteria were then adjusted to an OD_{600} of 0.2, which is equivalent to $1x10^8$ colony forming units (CFU)/mL. Then, the optical density-adjusted bacteria were centrifuged at 10,000 x *g* for 3 minutes and resuspended in 80% of the original volume Hanks Buffered Salt Solution with calcium and magnesium (HBSS+/+; Life Technologies, Inc.) [v/v] and 10% of the original volume 1 mg/mL DNA from salmon testes (EMD Millipore, Inc.) in HyClone Molecular Biology Grade Water (Thermo Fisher Scientific, Inc.) [v/v]. DNA from salmon testes was used to block unspecific binding of aptamers to bacteria. Then, 45-90 μL of bacterial suspension was mixed with 5-10 μL of 100 nM – 50 μM aptamer or alphamer in a round- or V-bottom 96-well plate (Corning, Inc.) and incubated for 30 – 45 minutes in normal atmosphere at 37°C. In some experiments, the 96-well plates were pre-blocked with casein blocking buffer (Thermo Fisher Scientific, Inc.) and then washed three times with assay buffer before adding aptamers/alphamers and GAS cells to the wells.

After the incubation of bacteria and aptamers or alphamers was completed, 150 μL of ice-cold HBSS+/+ was added on top of each sample, the plate was centrifuged at 3,220 x *g* for 5 minutes, and the samples were washed twice with 200 μL of ice-cold HBSS+/+ and resuspended in 300 μL of HBSS+/+ for flow cytometry analysis. 10,000 to 20,000 gated events of each sample were recorded with the following settings on CellQuest software: Forward light scatter (FSC): E00 (log); Side light scatter (SSC): 445 (log); and Fluorescence channel-1 (FL-1). FACS data were then analyzed using FlowJo (Tree Star, Inc.).

Molecular biology techniques

To obtain DNA templates for colony polymerase chain reactions (cPCRs), GAS M1T1 5448, GAS M1T1 5448 *emm1* knockout mutant, and GAS M1T1 5448 *emm1* knockout pDCerm-*emm1* complemented mutant colonies were resuspended in a 1.5 mL centrifuge tubes (Thermo Fisher Scientific, Inc.) in 15 μL of Milli-Q water (EMD Millipore) and the tubes heated in a conventional microwave for 3 minutes.

Genomic DNA from the above strains was isolated using Bactozol Bacterial DNA Isolation Kit (Molecular Research Center, Inc.). Modified Bactozol Enzyme Solution Lysis Protocol for streptococcal cells was followed per manufacturer's instructions.

To lyse the bacteria: Bacterial pellets were obtained by sedimenting 1.5 mL of bacterial overnight suspension at 6,000 x *g* for 4 minutes at room temperature; supernatants were decanted and pellets resuspended in 100 μL of Alternate Enzyme Solution (5 μL of 20 mg/mL proteinase K (Sigma-Aldrich, Inc.); 2 μL of mutanolysin at 25,000 units/mL (Sigma-Aldrich, Inc.); and 93 μL of Bactozol Enzyme Dilution Buffer). Samples were incubated for 90 minutes at 45°C with periodic mixing; 10 μL of 10x Bactozol Enzyme Solution was added after incubation. Subsequently, samples were gently vortexed and incubated for an additional 60 minutes at 45°C.

To solubilize the lysates: the samples were mixed 25 times with a pipet; 400 μL of DNAzol (Life Technologies, Inc.) was added to the lysates and the samples incubated for 15 minutes at 45°C.

To precipitate the DNA: 300 μL of 100% ethanol was added to the lysates; the lysate samples were mixed by inversion for 15 seconds and stored for 5 minutes at

room temperature; the DNA was sedimented by centrifugation at 3,000 x *g* for 4 minutes at room temperature.

To wash the DNA: the supernatants were decanted and the residual fluid was removed with a pipet; the DNA pellets were washed with 1.5 mL of 75% ethanol by vortexing; the samples were stored for 2 minutes at room temperature to allow the DNA precipitates to sediment; the supernatants were decanted; a second wash was performed similarly; the residual ethanol was removed.

To solubilize the DNA: 300 μL of HyClone water was added to the DNA pellets; stored the DNA pellets for 15 minutes at room temperature; and pipetted the samples until the gelatinous DNA was fully dissolved.

To quantitate the extracted DNA: Absorbances at 260 nm and 280 nm were measured with a ND-1000 Spectrophotometer using NanoDrop software (Thermo Fisher Scientific, Inc.) and determined the $A_{260/280}$ ratio to be within the 1.6-1.8 range; the DNA concentration was calculated with one A_{260} unit equaling 50 μg of double stranded DNA/mL.

PCR was performed with Platinum Blue PCR Supermix (Life Technologies, Inc.) using a T100 Thermal Cycler (Bio-Rad Laboratories, Inc.) with the following setup: 1 minute at 95°C; 20 cycles of 95°C for 15 seconds (denaturing), 55°C for 30 seconds (annealing), and 72°C for 2 minutes (extending); 5 minutes at 72°C; and 60 minutes at 4°C.

DNA gel electrophoresis

1.5% agarose gels were made in Tris-acetate-EDTA (TAE) buffer and GeneRuler 1 kb DNA ladder was used as a molecular-weight size marker. The gels were stained with ethidium bromide and visualized with a standard transilluminator. Anything that came in contact with ethidium bromide was disposed of appropriately. The *emm1* oligonucleotide primers used were specific for a 1.7-kb fragment containing 460 bp upstream of the *emm1* gene (Lauth-*emm1*-ext forward primer) and the first 1,203 bp of the *emm1* gene (Lauth-*emm*1-401 reverse primer; 15). Sequences of forward and reverse *emm1* primers and forward and reverse *cat* primers for 650-bp PCR amplicon of the *cat* gene from pACYC184 were: CGCAAAGAGGTTATCTTACCCACTC; CCGACTGGTTCTCTCTTGATGTTC; ATGGAGAAAAAAATCACTGGATATACCAC; and TTACGCCCCGCCCTGCCACTCATCGCAGT.

M1 protein and derived truncated constructs

His_6-tagged recombinant M1 protein and its truncated variants were provided by Dr. Partho Ghosh (Department of Chemistry and Biochemistry, University of California San Diego, La Jolla, CA). The protein constructs were: M1 protein AB (14 mg/mL and 20 mg/mL), M1 protein HC (13 mg/mL and 19 mg/mL), M1 protein BC (20 mg/mL), M1 protein SCD-his (4.0 mg/mL), and M1 WT-his (3.7 mg/mL). M1 protein and its fragments were suspended in low Tris pH 8, PBS, and/or NaCl and stored frozen at -80°C. A schematic of the used GAS M1 protein variants are show in **Figure 3**.

GAS M1T1 5448 lysate was also prepared, which was obtained after enzymatically lysing the bacteria with 500 units of mutanolysin (Sigma-Aldrich, Inc.). A second batch of the lysate was prepared by centrifuging 10 mL of bacteria in THB at 3,220 x *g* for 5 minutes, washing twice with 5 mL of DPBS, and resuspending in 500 μL HyClone water and 100 μL of mutanolysin at 5,000 unit/mL. The suspension was incubated for 2 hours at 60°C in a heating block to lyse the bacteria.

Enzyme-linked immunosorbent assay (ELISA): M1 protein

Flow cytometry experiments suggested that the target antigen of aptamers 20A24P is the M1 protein, a key virulence factor and the basis for serotyping of GAS strains (21). ELISA was performed with biotinylated aptamers (20A24P-BioTEG and RAND-80-BioTEG) thereafter to confirm that the target antigen of aptamer 20A24P was indeed the M1 protein. In general, ELISA experiments were carried out as follows: Wells of an Immulon 4HBX 96-well flat bottom polystyrene plate (Thermo Fisher Scientific, Inc.) were coated with 50 μL of duplicate samples of recombinant M1 protein and its truncated variants, lysate supernatant of GAS M1T1 5448, and negative control proteins (His-tagged PbSPECT Purified) and/or bovine serum albumin (BSA; Sigma-Aldrich, Inc.). All proteins were used at 20 μg/mL in DPBS. The plate was covered with a plate sealing tape (Thermo Fisher Scientific, Inc.) and incubated for 90 minutes at 37°C or overnight at 4°C.

Then, the coating solution was discarded and the wells were washed twice with 200 μL of DPBS. To block unspecific protein and nucleic acid binding sites, each well was blocked with 200 μL of Casein Blocking Buffer: 1% (w/v) casein in 100 mM

$NaPO_4$ and 150 mM NaCl at pH 7.4 containing Kathon Anti-microbial Agent (Thermo Scientific, Inc.) and 5 mg/mL DNA from salmon testes added as powder. The plate was covered with a plate sealing tape and incubated for 90 minutes at 37°C. Then, the wells were washed twice with 200 µL of HBSS+/+. Then, 50 µL of biotinylated aptamer 20A24P or RAND-80 at 1 µM end concentration (10% aptamer at 10 µM in aptamer vehicle (HyClone water) and 90% HBSS+/+) or aptamer vehicle with HBSS+/+ was added to duplicate well samples per protein. The plate was covered with a plate sealing tape again and incubated for 60 minutes at room temperature with 250 rpm horizontal shaking. Subsequently, the wells were washed with HBSS+/+ as above.

Then, protein-bound biotinylated aptamers were detected with horseradish peroxidase (HRP)-conjugated streptavidin (R&D Systems, Inc.) 1/200 diluted in HBSS+/+. 75 µL of diluted streptavidin was added to each washed well and the plate was incubated for 60 minutes at 37°C. Then, the wells were washed three times with 200 µL HBSS+/+. 100 µL of substrate solution (3,3'-5,5'-Tetramethylbenzidine [TMB]) (eBioscience, Inc.) was added to each well. After 10 minutes of color development protected from light at room temperature, 100 µL of stop solution (0.2 N sulfuric acid) was added to each well. Finally, the absorbance of each well was measured at 450 nm with VersaMax ELISA Microplate Reader using Softmax Pro software (Molecular Devices, Inc.).

DC Protein Assay: M1 protein

DC Protein Assay (Bio-Rad Laboratories, Inc.), a modified Lowry colorimetric assay, was performed to determine protein concentrations for ELISAs. Microplate assay protocol was followed per manufacturer's instructions: 20 μL of reagent S was added to each mL of reagent A (reagent A'); 3-5 dilutions of a protein standard were prepared; 5 μL of standards and samples were pipetted into a 96-well round-bottom plate; 25 μL of reagent A' was added to each well; 200 μL of reagent B was added to each well; reagents were gently mixed; and after 15 minutes, absorbances were measured at 750 nm.

Flow cytometry: recognition of GAS-bound FAM-labeled aptamer by anti-fluorescein antibody

Prior to testing the binding of α20A24P to GAS M1T1 5448 and its ability to act as an immune linker molecule, recognition of GAS-bound FAM-labeled aptamer (5'-FAM-20A24P) by immunoglobulin was tested using primary antibody 1 μg/mL mouse-derived anti-FITC IgG_{2a} monoclonal antibody (mAb; GenWay Biotech, Inc.), 1 μg/mL mouse-derived IgG_{2a} isotype mAb antibody control (Life Technologies, Inc.), or HBSS+/+ antibody vehicle control, and secondary detection antibody 4 μg/mL Alexa Fluor 647 goat-derived anti-mouse IgG (Life Technologies, Inc.) or HBSS+/+ as antibody vehicle control. All antibodies were diluted in HBSS+/+. Flow cytometer samples were prepared as described above; however, instead of resuspending in 300 μL HBSS+/+ after incubation with the aptamers, bacteria were resuspended in 100 μL primary antibody (anti-FITC mAb, isotype mAb, or HBSS+/+), incubated for 1 hour

at 4°C, washed twice with 200 μL HBSS+/+, resuspended in 100 μL secondary antibody (Alexa Fluor 647 IgG or HBSS+/+), incubated for 1 hour at 4°C protected from light, washed twice with 200 μL HBSS+/+, and then resuspended in 300 μL HBSS+/+. In addition to the instrument settings on CellQuest software used to detect aptamer binding, FL-4 channel was also measured to detect aptamer-, primary antibody-, and secondary antibody-bound GAS bacteria.

Flow cytometry: GAS alphamer as an immune linker molecule

Recognition of GAS-bound, 5'-alpha-Gal-20A24P-FAM-3', below referred to as α20A24P, to GAS M1T1 5448 was tested by incubating anti-alpha-Gal antibodies and fluorescently labeled anti-human or -mouse IgG or anti-mouse IgM secondary antibodies. The primary antibodies used were: human intravenous immunoglobulin (hIVIG), M86 mouse-derived anti-alpha-Gal polyclonal IgG, and M86 mouse-derived anti-alpha-Gal polyclonal IgM. The secondary detection antibodies used were: 4 μg/mL Alexa Fluor 647 goat-derived anti-human and anti-mouse IgG and anti-mouse IgM (Life Technologies, Inc.). HBSS+/+ was used as antibody vehicle control for both antibodies. Anti-alpha-Gal M86 antibodies were provided by Dr. Uri Galili (University of Massachusetts Medical School, Worcester, MA) and all antibodies were diluted in HBSS+/+.

Flow cytometry samples were prepared in an identical fashion as above, with alphamers instead of aptamers and corresponding antibodies. In short, GAS bacteria were incubated with alphamers or vehicle; washed twice with DPBS (centrifugation at 10,000 x *g* for 3 minutes); incubated with primary antibody; washed twice with

HBSS+/+; incubated with secondary antibody; washed twice with and resuspended in HBSS+/+. Alphamer-recognition flow cytometer samples were prepared and measured as FAM-labeled aptamer-recognition flow cytometer samples were performed.

Collection of plasma and serum from BALB/c GT$^{-/-}$ mice

BALB/c GT$^{-/-}$ mice with inactivated alpha 1,3-galactosyltransferase gene are deficient in the production of the alpha-Gal epitope (22) and thus mimic the situation in humans. BALB/c GT$^{-/-}$ mice were anesthetized with isoflurane and blood samples were collected by terminal heart puncture. For collection of mouse serum, blood was allowed to clot in sterile 1.5-mL microcentrifuge tubes. For collection of mouse plasma, blood was stored in sterile Microtainer tubes containing EDTA (Becton, Dickinson, and Company, Inc.) to avoid clotting. Blood samples were centrifuged for 10 minutes at 2,000 x *g* to separate plasma or serum from blood cells. After centrifugation, supernatants containing plasma or serum were collected and centrifuged for 10 minutes at 3,000 x *g* for further separation. Plasma or serum samples were pooled, aliquoted in appropriate portions, and stored in -80°C after shock freezing with dry ice.

Baseline deposition of complement by mouse plasma or serum and complement deposition assay (CDA)

The following GAS strains were tested for their background levels of complement deposition by mouse plasma or serum: GAS M1T1 5448, GAS M1T1

5448 AP, GAS M3 20224, GAS M4, GAS M11 NS414, GAS M12 NS488, GAS M49 NZ131, and GAS M77 NS236. For each strain, THB was inoculated with colonies of the respective strains from THA plates and incubated overnight at 37°C in normal atmosphere incubator. Then, bacteria were washed twice with DPBS with centrifugation at 10,000 x *g* for 3 minutes and the OD_{600} of each culture was measured 1:10 diluted in DPBS.

Bacterial cells were adjusted to an OD_{600} of 1.0 in DPBS, which is estimated to be equivalent to $5x10^8$ CFU/mL. In duplicates, 45 μL samples of bacteria were put in wells of a V-bottom 96-well plate and centrifuged for 5 minutes at 3,220 x *g* to pellet the bacterial cells. For CDA, bacteria were incubated with 5'-alpha-Gal-20A24P-FAM-3', 5'-alpha-Gal-RAND-80-FAM-3', or alphamer vehicle for 45 minutes at 37°C in a normal atmosphere incubator; for measuring the baseline deposition of complement, this incubation step was skipped. The samples were washed twice with DPBS, resuspended in 0-10% mouse plasma or serum in HBSS+/+, and then incubated for 5-45 minutes at 37°C with 225 rpm shaking.

After incubation, ice-cold HBSS+/+ was added to each well to stop the deposition reaction. The samples were then washed twice with ice-cold HBSS+/+ with 10% heat-inactivated fetal bovine serum (FBS; Thermo Fisher Scientific, Inc.) and resuspended in PE-labeled rat anti-mouse/human C3/C3b/iC3b mAb 1:100 diluted in HBSS+/+ (Cedarlane Laboratories, Inc.). The samples were protected from light and incubated for 60 minutes at 4°C, and resuspended in ice-cold HBSS+/+ after washing twice. The deposition of complement component C3b onto the bacterial surface was assessed by flow cytometry at FL2-H channel for anti-C3b mAb.

Isolation of human polymorphonuclear neutrophils (hPMNs)

Blood was drawn from healthy volunteers and collected with heparin (Fresenius Kabi USA, LLC) and a Vacutainer butterfly needle (Becton, Dickinson, and Company, Inc.) in a 60-mL Luer-lock disposable syringe (Henke-Sass Wolf). Blood was slowly layered on top of an equal volume of Polymorph solution (Axis-Shield, PLC) in 15 mL Falcon conical centrifuge tubes (Corning, Inc.). The tubes were then centrifuged at 520 x *g* for 40 minutes at room temperature with brake off. After centrifugation, blood and medium were separated according to the density gradient medium, from top to bottom: plasma, peripheral mononuclear cells (PBMCs), medium, polymorphonuclear neutrophils, medium, and sedimented erythrocytes.

Plasma, monocytes, and medium layers were aspirated, and the PMN layer was collected and put in a 50 mL Falcon conical centrifuge tube (Corning, Inc.). The tube was filled up to 50 mL with refrigerated DPBS and was centrifuged at 520 x *g* for 8 minutes with brake on. All centrifugation steps from here on were at 520 x *g* for 8 minutes with brake on. The pelleted cells were resuspended in 5 mL of HyClone water and incubated for at room temperature for 25 seconds to lyse the erythrocytes.

Immediately following the lysing incubation, 45 mL of 4°C DPBS was added to the tube and centrifuged again. The lysis step was repeated until the pelleted cells no longer contained erythrocytes. After the final lysis step, cells were washed in 10 mL of DPBS and resuspended in 10 mL of DPBS. 20 μL of the cell suspension was added to 80 μL of DPBS and 100 μL of trypan blue (Life Technologies, Inc.) in a 2 mL siliconized microcentrifuge tube (Thermo Fisher Scientific, Inc.). The stained cells

were counted using a hematocytometer (Thermo Fisher Scientific, Inc.), where 10 μL of the cell suspension was pipetted between the counting chamber and a cover-slip.

With a light microscope, stained cells in all four corner square grids were counted and averaged; the cell concentration was determined after calculating the dilution factor. During the counting step, the remaining 10 mL of cells in DPBS was centrifuged and resuspended in appropriate volume of HBSS+/+ per multiplicity of infection (MOI) tested. The MOI in this thesis denotes the ratio of GAS bacteria to hPMNs.

Opsonophagocytosis assay (OPA)

Wells of a V-bottom 96-well plate were blocked by incubating with casein blocking buffer (Thermo Scientific, Inc.) at 37°C for at least 60 minutes. After blocking, the wells were washed three times with 200 μL of HBSS+/+. THB was inoculated with GAS M1T1 5448 and vortexed to fully resuspend the bacterial cells in the media. The GAS suspension was mixed 1:1 with THB containing 40 μg/mL calcein-AM (Life Technologies, Inc.). After incubating overnight at 37°C in a normal atmosphere incubator, GAS cells were green fluorescent as confirmed with a BX51 fluorescence microscope (Olympus Corp.). Bacteria were washed four times with DPBS (centrifuged at 10,000 x *g* for 3 minutes) and then resuspended in HBSS+/+. Optical density of the washed culture was measured 1:10 diluted in HBSS+/+ in a polystyrene cuvette at 600 nm (OD_{600}) with GENESYS 10UV-Vis Spectrophotometer, with HBSS+/+ as the blank. Per MOI, bacteria were adjusted to different CFU/mL

(estimated by OD_{600}, where $OD_{600} = 1$ is equivalent to $1x10^9$ CFU/mL) to accommodate for the number of hPMNs purified per assay and kept on ice.

Optical density-adjusted bacterial cells were taken from ice and warmed in 37°C water bath and 20 μL of bacterial suspension was mixed with 5 μL of aptamers (5'-FAM-20A24P or 5'-FAM-RAND-80) and aptamer vehicle or alphamers (5'-alpha-Gal-20A24P or 5'-alpha-Gal-RAND-80) and alphamer vehicle in a pre-blocked V-bottom 96-well plate and incubated for 15 minutes in normal atmosphere at 37°C. For cells incubated with aptamers or aptamer vehicle, 25 μL of 37°C-warmed mouse anti-FITC IgG_{2a} mAb, mouse IgG_{2a} isotype mAb, or antibody vehicle was added to appropriate wells and incubated for 15-30 minutes. For cells incubated with alphamers or alphamer vehicle, 25 μL of 37°C-warmed hIVIG, M86 IgG, or antibody vehicle was added instead.

Then, 50 μL of hPMNs typically at 2.5×10^7 cells/mL in HBSS+/+ was added to each well, and while the assay plate was protected from light, the samples were incubated for 20 minutes at 37°C with 225 rpm shaking. Afterwards the plate was placed on ice to stop the reaction. The samples were washed twice in ice-cold HBSS (centrifuged at 520 x *g*), the cells were resuspended in 10 μL 4°C HBSS+/+ and the plate was placed on ice. 1.5 μL of each cell suspension was mixed with 1.5 μL of 1 mg/mL ethidium bromide (Life Technologies, Inc.) on a microscope slide and covered with a cover slip. Using Axiovert 40 CFL fluorescence microscope (Carl Zeiss, Inc.), 100 – 200 live hPMNs were analyzed per sample for phagocytosis of GAS cells.

Opsonophagocytic killing assay (OPKA)

The protocol for OPKA was identical to that of OPA except for the following adjustments: THB was inoculated with GAS. After 24 hours of incubation at 37°C in normal atmosphere, the overnight culture was diluted to OD_{600} of 0.05 in fresh 1.5 mL THB. Typically, this GAS suspension was incubated for 10 hours to an OD_{600} of 1.0 and then the samples were prepared as described in OPA. In addition, instead of incubating bacterial cells with hPMNs, 5 µL of bacteria with hPMNs were taken upon mixing and diluted 1:10 in Cellgro Molecular Biology Grade Water (Corning, Inc.) to lyse phagocytes. The samples were serially diluted to 1:1,000,000 and 5 µL of each dilution was dropped on a THA plate. Remaining samples were incubated at 37°C in normal atmosphere and 5 µL samples were taken, diluted, and plated at different time points. Colonies from the 5 µL drops were counted after overnight incubation to determine the CFU/mL at different time points. Duplicate to quadruplicate samples of each condition were collected in each experiment.

Whole blood killing assay (WBKA)

A streak of GAS colonies was inoculated in THB, serially diluted from 1:10 to 1:100,000 in THB, and incubated overnight at 37°C in normal atmosphere. OD_{600} of each suspension was measured and the culture with the optical density closest to 0.8 (late exponential phase) was chosen for the assay. Bacteria were washed twice with 4°C HBSS+/+ (centrifuged at 10,000 x *g* for 3 minutes), resuspended in HBSS+/+, and kept on ice. OD_{600} of the washed bacteria was measured again and the culture was adjusted to an OD_{600} of 0.075, which is estimated to be equivalent to $3.75x10^7$

CFU/mL. Two different inoculum concentrations – $3.75x10^7$ CFU/mL and $3.75x10^6$ CFU/mL – were tested in the assay.

To determine the initial concentrations of the bacteria (0-minutes time point), 24 μL of each culture was mixed with 6 μL of alphamer vehicle (DPBS) and 120 μL of HBSS+/+ in triplicate samples. Then, 10 μL of each sample was taken and serially diluted from 1:10 to 1:10,000 in HyClone water, and the CFU/mL was determined as described in OPKA.

Typically, to determine the CFU/mL at different time points, 24 μL of each culture was mixed with 6 μL of alphamers at 0.5 μM, 1.25 μM, 5 μM, or 12.5 μM or alphamer vehicle in triplicate samples and incubated for 15 minutes at 37°C. Then, 120 μL of heparinized human whole blood was added to each well of the assay plate; the plate was covered with a silicone plate sealing tape and incubated in a Labquake Rotisserie rotator (Thermo Scientific, Inc.) in a 37°C room. 10 μL of each sample was taken and the CFU/mL of each sample at different time points was determined.

Murine *in vivo* model of GAS necrotizing fasciitis

20 to 26 week-old female BALB/c $GT^{-/-}$ mice were used to establish an *in vivo* necrotizing fasciitis infection model with different concentrations of GAS M1T1 5448 bacteria. In some experiments, BALB/c $GT^{-/-}$ mice were passively administered with 1 mL 100 mg/mL hIVIG or antibody vehicle control (DPBS) via intraperitoneal injection 24 hours prior to infection with GAS bacteria.

A streak of GAS colonies were inoculated in 25 mL of THB and incubated overnight at 37°C in normal atmosphere incubator. The bacteria were then washed twice (centrifuged at 3,220 x *g*) and resuspended in DPBS. The bacterial cells were adjusted to OD_{600} of 4.0, which is estimated to be equivalent to $2x10^9$ CFU/mL. A portion of the bacterial suspension was diluted 1:1,000,000 in DPBS and plated on THA plates to determine the actual CFU/mL.

The remaining cells were then adjusted to $1x10^7$ CFU/mL, $1x10^8$ CFU/mL, and $1x10^9$ CFU/mL in DPBS with 1 mg/mL Cytodex microcarrier beads and kept on ice. Mice were anesthetized with 3% isoflurane (Piramal Enterprises, Ltd.) at a flow rate of 2L/min oxygen using VetEquip vaporizer (VetEquip, Inc.) and their dorsal flanks were shaved using a standard electric shaver. In the order of increasing bacterial dose, 100 μL of each suspension was subcutaneously injected in upper right, lower left, and lower right flanks of mice.

96 hours after infection, mice were euthanized by CO_2 inhalation and the infected sites were excised and put in pre-weighed 2.0 mL homogenization tubes (Sarstedt, Inc.) with 750 μL DPBS and 500 μL 1.0-mm Zirconia/Silica Beads (Bio Spec Products, Inc.). Using MagNA Lyser (F. Hoffmann-La Roche, Ltd), skin samples were homogenized for 2x1 minute at 6,000 rpm with 1 minute cooling on ice. Homogenized samples were serially diluted to 10^{-6} and 5 μL of each dilution was dropped on THA plates to determine CFU/mL for each infected site.

Ethics permissions. Permission to collect human blood under informed consent was approved by the UCSD Human Research Protection Program. All animal experiments

were conducted according to the guidelines approved by the UCSD Institutional Animal Care and Use Committee.

RESULTS

Identification of lead aptamer

9 published aptamers specific for Gram-positive bacteria group A *Streptococcus* (GAS; 13) were screened to identify a lead aptamer candidate for a proof-of-concept (POC) study for alphamer-mediated therapy. To that aim, 5'-FAM labeled green fluorescent aptamers were synthesized and tested for binding to live streptococci by flow cytometry.

In the original publication by Hamula *et al.* (13), the GAS aptamers were described to bind to bacteria in "binding buffer" – 1 x BB; 50 mM Tris-HCl (pH 7.4), 5 mM KCl, 100 mM NaCl, and 1 mM $MgCl_2$. Bindings of the nine, 5'-FAM-labeled DNA aptamers (see **Fig. 2** for secondary structures) in binding buffer were tested in flow cytometry experiments with live, stationary phase GAS M1 SF370 bacteria. Fluorescence level of aptamer compared to those of negative control aptamer and aptamer vehicle treated GAS cells was taken to represent the binding strength of an aptamer. GAS SF370 cells incubated with 5'-FAM-20A24P, an 80-nt fluorescent aptamer with reported binding dissociation constant (K_d) of 9 ± 1 nM (13), showed the greatest gated fluorescence level above that of streptococci exposed to FAM-labeled RAND-80, a 80-nt negative control aptamer, as well as aptamer vehicle (binding buffer with HyClone water; **Fig. 4**). 5'-FAM-20A24P also bound well to GAS cells in Hank's Balanced Salt Solution with or without calcium and magnesium (HBSS+/+ and HBSS-/-, respectively), Dulbecco's PBS without calcium and magnesium (DPBS),

and RPMI-1640 (data not shown). Most of the binding experiments described below were performed with HBSS+/+.

Binding of 20A24P was not dependent on the 5'-FAM fluorescence tag, as 3'-FAM-labeled 20A24P showed equivalent binding to GAS bacteria. 20A24P was therefore prioritized for further characterizations and POC experiments.

Broad spectrum binding of 20A24P

Confirming the results reported in the Hamula *et al.* publication (13), 5'-FAM-20A24P and 5'-FAM-20A24P.A3 aptamers demonstrated broad spectrum binding to GAS and significantly bound to GAS strains of clinically relevant serotypes: GAS M1 SF370 (**Fig. 4**), GAS M1 5448, GAS M3 20224, GAS M4, GAS M12 NS488, and GAS M77 NS236 (**Fig. 5**).

Truncation enhances binding strength of 20A24P

Aptamers are usually generated from SELEX process with primer regions containing fixed sequences to aid the amplification process (12). Often, these primer regions do not contribute to the target-binding domain of an aptamer and therefore can be truncated to minimize the aptamer sequence. For 20A24P, a full-length, 80-nt aptamer with 20-nt fixed sequence on each end, several truncated variants were produced in an effort to reduce the aptamer sequence to the minimal target-binding domain.

Of the seven truncated aptamers tested, the A3 variant of 52-nt length (20A24P.A3) showed the greatest binding strength, which was even greater than that

of the parental 20A24P aptamer (**Fig. 6**). With enhanced binding, the truncated A3 variant was tested in parallel with the parental aptamer in aptamer binding studies. Interestingly, it was observed later in functional studies that the truncated variant lost its binding potential when its 3' end was altered, for example by conjugating the fluorescein molecule to the 3' end (data not shown).

Loss-gain of 20A24P binding with *emm1*

20A24P was selected from SELEX process with live, whole GAS cells instead of a specific target molecule (e.g. hyaluronic acid capsule; 13). The target antigen of 20A24P was therefore unknown, but likely a cell surface-associated antigen. Both aptamers showed equivalent binding to stationary phase wild-type GAS M1T1 5448 and a capsule deficient Δ*hasA* mutant, indicating the GAS hyaluronic acid capsule itself was not the aptamer target, and that expression of capsule did not block aptamer access to its molecular target on the GAS surface in the stationary phase (data not shown). The next antigen tested was the M1 protein, which acts as the basis for serotyping of GAS strains (21). The M1 protein is encoded by the *emm1* gene, and the bindings of 20A24P and 20A24P.A3 to GAS M1 5448 were therefore compared to those of GAS M1 5448 Δ*emm1*. 5'-FAM-20A24P and 5'-FAM-20A24P.A3 showed significant bindings to the wild-type strain, but failed to bind to the mutant strain. Binding was restored to a mutant strain complemented with a plasmid vector to express the *emm1* gene (**Fig. 7**). The loss-gain of binding with the *emm1* gene suggested that the target antigen of 20A24P was the M1 protein or a protein that required the expression of the *emm1* gene.

Molecular techniques confirm the mutagenesis of *emm1*

To verify that GAS M1 5448 Δ*emm1* strain used for the above-described experiments was indeed deficient for the *emm1* gene, DNA samples of the wild-type strain, the mutant strain, and the complemented mutant strain were extracted from a single colony of each strain. However, the DNA extraction method failed to provide sufficient yield for PCR analysis (data not shown). Genomic DNA extraction using Bactozol Bacterial DNA Isolation Kit, however, was successful in producing sufficient DNA samples for PCR analysis. Gel electrophoresis analysis showed that the wild-type strain had a slightly larger band (~1,600 bp) than the mutant and the complemented mutant strains when using the *emm1* gene specific primer pair *emm1* F and R, which is consistent with a partial *emm1* gene deletion that was reported by Lauth *et al*. (15; **Fig. 8**). Moreover, by using the forward and reverse primer pair *cat*F and *cat*R, respectively, it was verified that the mutant and the complemented mutant strains contained the *cat* chloramphenicol resistance gene cassette, which was used to inactivate the *emm1* by insertion mutagenesis. Finally, it was confirmed with the primer pairs *emm1* F/*cat* R and *emm1* R/*cat* F that the chloramphenicol resistance cassette was inserted in the *emm1* gene region as expected. Together, the PCR data conclusively showed on the genomic level that the strains used for determining aptamer binding were indeed GAS wild-type, the isogenic *emm1* mutant and the complemented mutant strains.

20A24P binds to recombinant M1 protein

To further establish the target antigen of 20A24P and 20A24P.A3, binding of a 3’ biotinylated version of the GAS aptamer 20A24P to recombinant M1 protein and truncated constructs of the protein was tested in a colorimetric enzyme-linked immunosorbent assay (ELISA), where aptamer binding would be result in a development of color from clear to yellow. Biotinylated aptamer 20A24P showed significant binding to the full-length M1 protein and SCD construct containing conserved regions C and D, whereas biotinylated negative control aptamer RAND-80 and aptamer vehicle did not (**Fig. 9**). Of note, biotinylated aptamer 20A24P weakly bound to other regions of the M1 protein, some of which are hypervariable (A) and variable (B) by nature and account for >100 M serotypes. The aptamer also weakly bound to the HC construct, which contains regions H (18 amino acids), A (74 amino acids), B (61 amino acids), S (31 amino acids) and the first 37 amino acids of the C region. Since 20A24P weakly bound to the HC construct yet strongly bound to the SCD construct. Therefore, the specific target antigen of 20A24P is likely the latter 67 amino acids of the C region (104 amino acids), the D region (123 amino acids), or both.

Growth phase dependency of 20A24P

The initial aptamer binding studies with 20A24P were performed with overnight stationary phase GAS THB cultures. To determine the optimal growth phase for 20A24P binding, GAS M1 5448 cells at different phases of growth were harvested (**Fig. 10**). 5’-FAM-20A24P and 5’-FAM-20A24P.A3 selectively bound to GAS

cultures of at least late exponential phase (OD_{600} of >0.8) and therefore demonstrated a growth phase-dependent binding pattern (**Fig. 11**).

Expression and accessibility of M1 protein

The *emm1* gene is constitutively expressed in all growth phases of GAS (24), and therefore binding of 20A24P would have been expected for all optical density samples. One possible reason for the absence of binding in earlier growth phases (OD_{600} of <0.8) was that selective production of the hyaluronic acid (HA) capsule may be blocking the M1 protein from 20A24P until late exponential phase, when the *hasA* gene, which encodes the HA synthase, is no longer expressed (24). To test for the effect of the HA capsule on 20A24P binding, the binding of 20A24P to the following GAS strains were tested: GAS M1 5448 Δ*hasA*, GAS M1 SF370, and GAS M1 5448 AP.

The first strain is a nonencapsulated mutant strain, which cannot synthesize the HA capsule. If the HA capsule was truly blocking the aptamer binding, 20A24P would be expected to bind to the nonencapsulated bacteria at all growth phases. However, identical binding pattern was observed with the *hasA* knockout mutant strain as with the wild-type strain, where aptamers 5'-FAM-20A24P and 5'-FAM-20A24P.A3 showed significant bindings to GAS cells in late exponential phase and stationary phase, but not in any earlier growth phase (**Fig. 12A**).

To further confirm that the absence of the HA capsule does not lead to increased 20A24P binding, the same binding test was performed with GAS M1 SF370 strain, a non-M1T1 clonal isolate that produces much less HA capsule than a M1T1

clonal strain (25). 20A24P aptamer significantly bound to stationary-phase SF370 cells, and therefore confirmed that the reduction of the HA capsule does not affect or enhance 20A24P binding to the M1 protein (**Fig. 12B**).

In addition, binding of 20A24P to GAS M1 5448 AP, an animal-passaged strain with an overexpression of the *hasA* gene, was tested to see whether the increased encapsulation would decrease 20A24P binding. 20A24P aptamer bound to the AP strain as well (**Fig. 12C**), and it was concluded that the HA capsule does not affect the binding of 20A24P to the M1 protein.

Next, the effect of the SpeB cysteine protease on 20A24P binding was tested with GAS M1 5448 Δ*speB* mutant strain. The *speB* gene, responsible for synthesis of the SpeB, is expressed only in stationary phase and the protease was previously described to cleave the M1 protein (26). Therefore, it was suggested that the M1 protein required proteolytic cleavage by the SpeB prior to being available for 20A24P binding. 5'-FAM-20A24P and 5'-FAM-20A24P.A3 showed significant bindings to overnight broth culture of the mutant strain, indicating that the SpeB cysteine protease does not affect the binding of 20A24P to the M1 protein (**Fig. 12D**).

Lastly, the effect of the Sda1 DNase on 20A24P binding was tested with GAS M1 5448 Δ*sda1* mutant strain. The *sda1* gene is unique to the M1T1 genetic clonal isolate M1 5448 strain, and, as 5'-FAM-20A24P and 5'-FAM-20A24P.A3 are likely susceptible to degradation by nucleases, the effect of the gene's product the Sda1 DNase on 20A24P binding was crucial to explore. However, the binding pattern observed with the mutant strain was identical to that with the wild-type strain and

therefore it was determined that the Sda1 DNase does not affect the binding of 20A24P to the M1 protein (**Fig. 12E**).

In conclusion, the binding of 20A24P was not impeded by the HA capsule, the target antigen of the aptamer does not require protease processing by SpeB and the DNase Sda1 does not appear to impair the aptamer binding under tested conditions.

GAS-bound alphamer can be recognized by anti-alpha-Gal antibody

To test the mode-of-action (MOA) of the proposed alphamer-mediated therapy, the potential of an alphamer acting as an immune linker molecule was explored first with FITC fluorescein-labeled aptamer (5'-FAM-20A24P), mouse anti-FITC IgG_{2a} primary antibody, and fluorescent Alexa Fluor 647 goat anti-mouse IgG secondary antibody. Cell population with significant FL-1 fluorescence level represented GAS cells with bound aptamers while cell population with significant fluorescence levels of both FL-1 and FL-4 channels represented GAS cells with bound aptamers and antibodies (**Fig. 13**). There were no cells bound by antibodies without bound aptamers and all aptamers and the FITC molecule of 20A24P aptamer was specifically recognized by its specific antibody.

This experiment parallels the mode-of-action (MOA) of the proposed alphamer-mediated therapy where an alphamer would specifically bind to the target pathogen, and the conjugated alpha-Gal epitope would be recognized by anti-alpha-Gal antibodies that are abundantly produced in the body.

The next step was then to test the recruitment of anti-alpha-Gal antibodies to GAS cells by alphamers. As a consistent high titer source of anti-alpha-Gal antibodies,

polyclonal mouse IgM and IgG purified from the pooled serum from transgenic $GT^{-/-}$ mice expressing the variable portion of the mouse monoclonal anti-alpha-Gal antibody M86 (Ref.) were utilized. GAS cells were pre-incubated with 3'-FAM alphamer α20A24P, 3'-FAM control alphamer αRAND-80 or vehicle. The samples were then mixed with mouse polyclonal IgM, or IgG or buffer only, and surface bound IgM and IgG were detected with Alexa Fluor 647 labeled secondary anti-mouse IgM and IgG antibodies, respectively. By flow cytometry, both alphamer binding (FL-1 channel) and secondary antibody binding (FL-4 channel) could be simultaneously measured. As seen in the leftmost FL-1 histogram overlay in **Figure 14**, 3'-FAM-α20A24P bound well to live GAS, whereas the αRAND-80 treated cells showed only background FL-1 fluorescence pattern comparable to vehicle treated bacteria. Strongly enhanced levels of mouse IgG binding could be detected on 3'-FAM-α20A24P treated GAS (leftmost FL-4 histogram in **Figure 14**) indicating that IgG antibody recognized the GAS alphamer on the streptococcal surface. As negative controls, bacteria treated with GAS alphamer, negative control alphamer or vehicle, were probed with secondary antibodies in the absence of mouse polyclonal IgG. In this experiment, α20A24P bound well to GAS in the absence of polyclonal IgG (**Fig. 14**), but no secondary antibody signal was observed (**Fig. 14**), ruling out non-specific secondary antibody binding to 3'-FAM-α20A24P treated GAS. Similar results were obtained with mouse polyclonal IgM which bound only to 3'-FAM-α20A24P treated GAS. Experiments performed by my collaborators after the completion of the thesis demonstrated that the alpha-Gal epitope was required for the recruitment of mouse antibodies to the bacterial

surface (Sascha Kristian, personal communications; data not shown) indicating that anti-alpha-Gal antibodies specifically bound to the bacteria.

When hIVIG was used as the source of anti-alpha-Gal antibodies, α20A24P treatment did not enhance deposition of anti-alpha-Gal antibodies when compared to αRAND-80 and alphamer vehicle control treatments, because of high background hIVIG binding to the bacteria (data not shown).

Baseline level of complement deposition by mouse serum and the effect of alphamer treatment

After establishing the MOA of the proposed alphamer-mediated therapy, we then went on to test the effect of alphamer treatment in functional activity assays. The first functional activity assay that we tried was complement deposition assay (CDA), where we had hoped to see an increased deposition of complement components with α20A24P treatment. We established a CDA model where GAS bacteria were sequentially incubated with alphamers, a source of anti-alpha-Gal antibodies, and secondary PE-labeled detection antibodies. GAS bacteria were then subjected to FL-1 and FL-2 fluorescence channels to measure alphamer binding and anti-C3b detection antibody, respectively.

The initial CDA experiments with GAS M1 5448 strain and pooled mouse plasma or serum showed that the background level of complement deposition by plasma or serum was high, and all treatments (α20A24P, αRAND-80, and alphamer vehicle) showed similar fluorescence levels at FL-2 (data not shown). To find a GAS strain with lower background deposition of complement components, CDAs without

the alphamer incubation step were performed with GAS M1 5448 AP, GAS M3 20224, GAS M4, GAS M11 NS414, GAS M12 NS488, GAS M49 NZ131, and GAS M77 NS236 strains. The baseline level of complement deposition for each strain was not established, as many of the findings were not reproducible (data not shown).

GAS M1 5448 strain was reselected as the model strain and many of the experimental settings instead were modified in an effort to establish the baseline level of complement deposition. Different plasma or serum incubation times (5, 15, 30, or 45 minutes), a range of plasma or serum (0-10%), as well as new batches of plasma and serum were tested, but we did not observe a dose-dependent pattern of complement deposition by mouse plasma or serum detected by anti-C3b complement component antibody (**Fig. 15**).

α20A24P confers uptake of GAS by human neutrophils

The next functional activity assay we tried was opsonophagocytosis assay (OPA), where alphamer treatment may enhance the uptake of GAS bacteria by human neutrophils (hPMNs). We first prepared green fluorescent GAS bacteria by exposing the bacteria to calcein-AM during overnight incubation. Green-fluorescent GAS bacteria could be counterstained by the nucleic acid stain ethidium bromide, which produced red-fluorescent bacteria. Therefore when GAS bacteria were inside viable PMN cells (intracellular), bacteria remained green-fluorescent, while those outside PMN cells (extracellular) were exposed to the intercalating agent and turned red-fluorescent (**Fig. 16**).

Preliminary OPA experiments with 5' FAM-labeled aptamers and IgG antibodies showed promising results where 20A24P- and anti-FITC IgG_{2a}-treatment led to increased uptake of GAS bacteria by hPMNs compared to control samples (RAND-80, aptamer vehicle, isotype IgG_{2a}, or antibody vehicle treatment; data not shown).

The next OPA experiments with alphamers established the first POC of alphamer-mediated therapy, where α20A24P increased the function of human neutrophils by promoting the uptake of GAS bacteria. hPMNs treated with α20A24P nearly doubled the uptake of hypervirulent GAS M1 5448 bacteria when compared to hPMNs treated with controls (**Fig. 17**). The increased function of phagocytes suggests that the anti-alpha-Gal antibody bound to α20A24P on the GAS cell surface was recognized by Fc receptors on hPMNs inducing phagocytosis of the bacteria. In addition, comparison of the opsonophagocytic capacity of 20A24P aptamer to α20A24P showed that the alpha-Gal epitope is required for the increased function of hPMNs (**Fig. 18**).

Opsonophagocytic killing capacity of human neutrophils and the effect of alphamer treatment

After showing increased uptake of GAS bacteria by hPMNs with α20A24P treatment, we then tested to see if the increased function of hPMNs translated to improved killing of GAS mediated by α20A24P. Opsonophagocytic killing assays (OPKAs) with GAS M1 5448 bacteria and hPMNs, however, showed that the assay conditions needed to be optimized, as GAS cells without hPMNs were reduced by 90%

in the assay medium as well (data not shown). Of note, GAS M1 SF370 bacteria did not die in the assay medium itself and subsequent experiments using the newly established OPKA with modified conditions demonstrated improved killing of GAS M1 SF370 bacteria by hPMNs with α20A24P treatment (Sascha Kristian, personal communications; data not shown).

Alphamer treatment impairs outgrowth of GAS in human blood

Next functional activity assay tested was whole blood killing assay (WBKA), where GAS M1 5448 bacteria were preincubated α20A24P, αRAND, or alphamer vehicle before incubating in whole blood drawn with heparin from healthy volunteers. While the administration of α20A24P did not lead to direct clearance of GAS M1 5448 bacteria in human whole blood, the alphamer treatment impaired outgrowth of the hypervirulent strain that was otherwise observed in control-treated samples (**Fig. 19**). We determined that the newly established assay could be further optimized to show a more pronounced effect of α20A24P on GAS bacteria killing by human whole blood.

Establishment of *in vivo* GAS infection model and increasing nuclease resistance of aptamers

Next, an *in vivo* necrotizing fasciitis GAS infection model was established with BALB/c $GT^{-/-}$ mice, which can be immunized with anti-alpha-Gal antibodies to mimic the human condition. 20 to 26 week-old female $GT^{-/-}$ mice were intraperitoneally injected with 1 mL 100 mg/mL hIVIG 24 hours prior to infection with late exponential

phase GAS M1 5448 bacteria. Each mouse was subcutaneously injected with three different loads of GAS bacteria at three different sites on its dorsal flank. Skin samples from the injection sites were harvested 96 hours after infection and surviving bacterial CFU/mL for each site was determined by plating serially diluted homogenized tissue samples on THA plates.

GAS bacteria recovered from each infection site was dependent on the initial load of bacteria, with approximately $1x10^3$ CFU/mL bacteria surviving from the low inoculum of $1x10^7$ CFU/mL, $1x10^7$ CFU/mL from the medium inoculum of $1x10^8$ CFU/mL, and $1x10^8$ CFU/mL from the high inoculum of $1x10^9$ CFU/mL (**Fig. 20**). Paralleling the recovered GAS bacteria CFU/mLs, a lesion and an abscess were observed at the high and medium inoculum infection sites, whereas no visible skin perturbation was noted at the low inoculum infection site (**Fig. 20**).

Finally, to improve aptamers' resistance to DNA nucleases that are to be found in an *in vivo* system, an inverted thymidine (dT) was conjugated to the 3' end of aptamers. Conjugation of a dT at the 3'd end of an aptamer creates a 3'-3' linkage, which makes the aptamer's 3' end unrecognizable by 3' exonucleases, increasing the aptamer's resistance to the 3' specific exonucleases. Binding pattern of 5' FAM-20A24P-dT 3' to GAS M1 5448 cells was identical to that without the inverted nucleotide (**Fig. 21**).

DISCUSSION

In this thesis project, we prioritized a published GAS-binding DNA aptamer, 20A24P (13), for a POC study with alphamers. We then characterized the binding of this aptamer to multiple serotype strains of GAS and identified the target antigen of the aptamer as the M protein. We were also able to enhance the binding capacity of 20A24P by truncating the 80-nt aptamer to a 52-nt variant. The alpha-Gal epitope was conjugated at 20A24P's 5' end to generate 20A24P alphamer (α20A24P), and binding tests determined that the alpha-Gal conjugate retained reactivity with GAS cells.

α20A24P was capable of recruiting mouse IgG and IgM antibodies to the streptococcal surface, which in turn promoted phagocytosis of bacteria by purified human neutrophils (hPMNs). In whole blood killing assays (WBKAs), α20A24P treatment did not lead to direct clearance of the hypervirulent GAS M1 5448 strain in human whole blood, but rather impaired the outgrowth of the bacteria. Other key functional *in vitro* activity assays, namely opsonophagocytic killing assays and complement deposition assays, were established in the thesis, where, upon future optimization, α20A24P could further establish the proof-of-concept (POC).

Lastly, *in vivo* necrotizing fasciitis mouse model was established with BALB/c $GT^{-/-}$ mice, which parallels the human condition of lacking the alpha-Gal epitope. These mice could then be immunized with human intravenous immunoglobulin (hIVIG) to produce an abundance of anti-alpha-Gal antibodies which then could be redirected upon α20A24P treatment to the infected sites.

Although 9 published aptamers were described to bind with remarkable dissociation constants (K_d) comparable to those of highly specific antibodies (e.g. 20A12P K_d = 25 ± 3 nM), it was surprising that only 20A24P showed promising binding detected via significant fluorescence shift over controls. The difference in binding pattern, however, may be due to the fact that the 9 aptamers were selected against a mixture of 10 M-type GAS strains (13). After prioritizing 20A24P as the lead candidate aptamer, we went on to truncate 20A24P, as other papers have reported increase of binding up to 200-fold (27). Initially, we were very pleased with the enhanced binding that we observed with truncated A3 variant (5'-FAM-20A24P.A3), but later noted the loss of binding when its 3' end was altered (data not shown). As our alphamer model for POC required both 5' and 3' ends for conjugations with the alpha-Gal epitope and a detection fluorescence tag, respectively, we reprioritized the full-length, parental 20A24P aptamer for our functional studies. Nevertheless, non-FAM labeled 5'-alpha-Gal 20A24P.A3 showed activity in phagocytosis studies.

Repeated flow cytometry results confirmed the binding of 20A24P to various strains of GAS, a broad spectrum binding which suggested that the specific target of 20A24P to be a highly conserved antigen. From binding studies of 20A24P to multiple knockout strains, we were able to narrow down the target antigen of 20A24P aptamer to the M1 protein, which is expressed by the *emm1* gene. Later, binding of 20A24P aptamer to recombinant M1 protein – specifically the highly conserved regions C and D – explained the broad spectrum binding pattern.

After observing the loss-gain of binding with the Δ*emm1* gene, we were puzzled however, by the growth-phase dependent binding pattern. The *emm1* gene is

constitutively expressed (24) and therefore we expected a growth-independent 20A24P binding rather than absence of significant binding until late exponential phase (~OD_{600} = 0.8). The reason for the absence of 20A24P binding to GAS of early- and mid-exponential growth phase bacteria remains unclear, but may be due to a number of possibilities, such as that sufficient M1 protein has to be accumulated throughout the bacteria's growth before it can be recognized by the aptamer. It is also possible that since a substantial amount of the lipoteichoic acid (LTA) is secreted from GAS as a result of turnover (28), the specific target antigen region(s) of the M1 protein become accessible by 20A24P in later growth phases. The surface charge of the bacteria was noted to change during its growth, and the ionic charges of the aptamer and the M1 protein may play an important role in the binding function as well (29).

After characterizing the binding of aptamer 20A24P, we then moved onto functional activity assays to establish POC of alphamer-mediated therapy. Prior to synthesizing FAM-labeled alphamers, a model of the alphamer binding and IgG recognition thereof GAS-bound alphamer was tested using fluorescent FAM tag as both a detection label and a recognition molecule. Binding of 5'-20A24P-FAM aptamer to GAS bacteria was detected at FL-1 channel and overlaid with fluorescence measured at FL-4 channel to show that IgG antibodies were bound to the aptamer, which was bound to our model bacteria GAS. These results were encouraging and showed that the experimental system designed for alphamer binding and subsequent recognition by IgG antibodies was working. After 3'-FAM-labeled, 5'-alpha-Gal-conjugated alphamers were synthesized, the same binding-recognition assay was

performed and confirmed that our experimental model could be expanded upon to test the effect of alphamer treatment subsequent recruitment of IgG and IgM antibodies.

The first functional activity assay performed was complement deposition assay (CDA), where the effect of alphamer treatment on deposition of complement component C3b was measured. Complement component C3b is known to bind to bacterial cell surface and aid in opsonization, and it was postulated that the presence of anti-alpha-Gal antibodies would lead to increased formation of the C1qrs complex, and, later deposition of the cleaved C3b component.

However, numerous CDA experiments showed failed to determine the baseline level of complement deposition by mouse plasma or serum. In addition, deposition of complement did not follow a dose-dependent pattern with mouse plasma or serum despite the fact that the differences in level of individual mouse serum or plasma was accounted for by pooling the collected volumes and thereby using a batch of serum or plasma for multiple experiments. One possible reason for the inconsistencies observed in CDAs may be due to the M1 protein, which limits C3b deposition by binding to complement regulator C4b-binding protein (30). Each experiment's inoculum of GAS may have produced different amounts of M1 protein to result in different levels of C3b deposition. After the CDA is optimized where the baseline level of complement deposition is determined, nucleases in serum should be accounted for with nuclease resistant aptamers or alphamers.

Opsonophagocytosis assay (OPA) experiments on the other hand showed a clear effect of alphamer treatment on phagocytosis of GAS bacteria by purified human neutrophils (hPMNs) in the presence of mouse or human IgG as source of anti-alpha-

Gal antibodies. Statistically significant increase in uptake of GAS cells by hPMNs has a critical immunologic implication, where redirecting of preexisting antibodies could counteract the antiphagocytic and immune-evading functions that GAS possesses. Ultimately on a larger context, the POC has been established and the alphamer treatment is promising for more extensive functional activity assays as well as *in vivo* administration.

The initial experiments with opsonophagocytic killing assay (OPKA) did not show any observable impact of alphamer treatment on hPMN-mediated killing of GAS cells and the two negative controls – incubated with control alphamer αRAND-80 and alphamer vehicle – showed drastically different results. Also, the GAS M1 5448 bacteria died in the assay medium in the absence of phagocytes making it difficult to see hPMN-dependent killing activity. After the work presented in this thesis was completed, the experimental settings of the newly established OPKA were further optimized. Specifically, GAS M1 SF370 was selected for phagocytic killing experiments. This strain did not die in the assay medium alone; moreover, α24A24P conferred enhanced phagocytic killing by hPMN as compared to the control alphamer or vehicle (Sascha Kristian, personal communication; data not shown).

The last functional activity assay undertaken was whole blood killing assay (WBKA), where alphamer treatment did not clear GAS cells, but rather impaired the outgrowth of the hypervirulent GAS M1 5448 bacteria. Nucleases found in human whole blood may be degrading the alphamers and therefore interfering with its potential activity. In addition, alphamer treatment may lead to direct clearance of bacteria or a more significant impairment of GAS growth with less virulent strains.

In future experiments, BALB/c $GT^{-/-}$ mice could be immunized with human intravenous immunoglobulin (hIVIG), which is commercially available, to produce an abundance of anti-alpha-Gal antibodies. Alphamer treatment in necrotizing fasciitis skin infection or even systemic GAS infection could show decrease in lesion formation in the former and increased survivability rate or clearance of infection in the latter setting.

The significance of this potential, novel anti-infective therapy is three-fold. First, administration of bacterium-specific alphamers could, at the least, reduce the disturbance of the beneficial host commensal microflora, a common side effect that commonly accompanies the use of broad-spectrum antibiotics. In addition, alphamers could target multi-drug-resistant (MDR) bacteria that are difficult to treat with standard of care antibiotics while keeping the propagation of antibiotic resistance at bay. Most importantly, alphamers, by the virtue of their simple mechanism of action (MOA) – guiding innate immune cells to bacteria that have evolved to evade them – can be reselected to counteract pathogens' evolutions.

For example if the target pathogenic species of an alphamers evolves to evade the drug binding, a new aptamer portion can be selected against the evolved strain, upon which the alpha-Gal epitope can be conjugated and a new alphamer that binds to the pathogen can be created. However, in foresight of such rise in resistance against alphamers, administration of cocktail of bacterium-specific alphamers with various conserved antigens as their binding targets (e.g. for *E. coli*: LPS, K surface antigen, and H flagellar antigen) should limit the probability of gaining resistance to any specific alphamer.

In summary, the data I presented in this thesis showed that alpha-Gal linked to a GAS specific DNA aptamer can label bacteria for recognition by pre-existing anti-alpha-Gal antibodies and can mediate host phagocytic uptake and limit GAS replication in human blood. Our preliminary proof-of-concept data raise the possibility that any other bacterial pathogen for which a specific alphamer could be designed could be targeted for recruitment of functional antibodies from human serum. Further exploration of this novel therapeutic approach of applying alpha-Gal technology to nuclease resistant aptamers specific for additional pathogens of critical importance to human medicine such as multi-drug resistant species is warranted.

TABLES

Table 1. Table of aptamers and alphamers used in the thesis with their sequences and modifications at 5’ and 3’ ends.

Aptamer	Sequence name	Sequence (5'-->3')	5' modification	3' modification
Fluorescent	15A3P	TTCACGGTAGCACGCATAGGGACAGCAAGCC CAAGCTGGGTGTGCAAGGTGAGGAGTGGGCA TCTGACCTCTGTGCTGCT	FAM	
Fluorescent	20A1P	TTCACGGTAGCACGCATAGGCAGAACGCACC CGCACACCTCCATCACTCGCATGCACCCCCA TCTGACCTCTGTGCTGCT	FAM	
Fluorescent	20A8	CCCCACGAATCGTTACTCTGGTCCTCTATTTC TCCTCCCC	FAM	
Fluorescent	20A8P	AGCAGCACAGAGGTCAGATGCCCCACGAATC GTTACTCTGGTCCTCTATTTCTCCTCCCCCT ATGCGTGCTACCGTGAA	FAM	
Fluorescent	20A9	CACACGCTGAAGAAACTGAGGTCGTAGGTTTT CTTCGGG	FAM	
Fluorescent	20A9P	AGCAGCACAGAGGTCAGATGCACACGCTGAAG AAACTGAGGTCGTAGGTTTTCTTCGGGCCTAT GCGTGCTACCGTGAA	FAM	
Fluorescent	20A12P	TTCACGGTAGCACGCATAGGGCCCGACACTC GTCCACCCGATACCTCTCATGTGTCCCCATCT GACCTCTGTGCTGCT	FAM	
Fluorescent	20A14P	AGCAGCACAGAGGTCAGATGGGCATGGGGAA GAGAAAGCGGGATAACTTCGTTACCGGGCCCT ATGCGTGCTACCGTGAA	FAM	
Fluorescent	20A24P	AGCAGCACAGAGGTCAGATGGGGGGAAGACA CAGAGAAAGGCCGGGGTGAAGTGTAGAGGCC TATGCGTGCTACCGTGAA	FAM	
Biotinylated	20A24P	AGCAGCACAGAGGTCAGATGGGGGGAAGACA CAGAGAAAGGCCGGGGTGAAGTGTAGAGGCC TATGCGTGCTACCGTGAA		BioTEG
Fluorescent inverted dT	20A24P	AGCAGCACAGAGGTCAGATGGGGGGAAGACA CAGAGAAAGGCCGGGGTGAAGTGTAGAGGCC TATGCGTGCTACCGTGAA	FAM	inverted dT

Table 1. Table of aptamers and alphamers used in the thesis with their sequences and modifications at 5’ and 3’ ends, continued.

Aptamer	Sequence name	Sequence (5'-->3')	5' modification	3' modification
Alphamer	20A24P	AGCAGCACAGAGGTCAGATGGGGGGAAGACA CAGAGAAAGGCCGGGGTGAAGTGTAGAGGCC TATGCGTGCTACCGTGAA	alpha-Gal	
Fluorescent alphamer	20A24P	AGCAGCACAGAGGTCAGATGGGGGGAAGACA CAGAGAAAGGCCGGGGTGAAGTGTAGAGGCC TATGCGTGCTACCGTGAA	alpha-Gal	FAM
Fluorescent random control	RAND-80	TTCACGGTAGCACGCATAGGGTGCAAGCTGAG GCAAGCAACAGCGGAGGTGCGTTGAGGGCAT CTGACCTCTGTGCTGCT	FAM	
Biotinylated random control	RAND-80	TTCACGGTAGCACGCATAGGGTGCAAGCTGAG GCAAGCAACAGCGGAGGTGCGTTGAGGGCAT CTGACCTCTGTGCTGCT		BioTEG
Fluorescent random control alphamer	RAND-80	TTCACGGTAGCACGCATAGGGTGCAAGCTGAG GCAAGCAACAGCGGAGGTGCGTTGAGGGCAT CTGACCTCTGTGCTGCT	alpha-Gal	FAM
Fluorescent truncated	20A24P_A2	AGCACAGAGGTCAGATGGGGGGAAGACACAGA GAAAGGCCGGGGTGAAGTGTAGAGGCCTATG CGTGCT	FAM	
Fluorescent truncated	20A24P_A3	AGGTCAGATGGGGGGAAGACACAGAGAAAGGC CGGGGTGAAGTGTAGAGGCC	FAM	
Fluorescent truncated alphamer	20A24P_A3	AGGTCAGATGGGGGGAAGACACAGAGAAAGGC CGGGGTGAAGTGTAGAGGCC	alpha-Gal	FAM
Fluorescent truncated	20A24P_A4	AGGTCAGATGGGGGGAAGACACAGAGAAAGGC CGGGGTGAAGTGTAGAGGCC	FAM	
Fluorescent truncated	20A24P_A5	AGGTCAGATGGGGGGAAGACACAGAGAAAGGC CGGGGTGAAGTGTAGAGGCCA	FAM	
Fluorescent truncated	20A24P_A6	AAGGCCGGGGTGAAGTGTAGAGGCCTA	FAM	
Fluorescent truncated	20A24P_A8	TGGGGGGAAGACACAGAGAAAGGCCGGGGTG AAGTGTAGAGGC	FAM	
Fluorescent truncated	20A24P_A9	AGAGGTCAGATGGGGGGAAGACACAGAGAAAG GCCGGGGTGAAGTGTAGAGGCCTAT	FAM	
Fluorescent truncated random control	RAND-52	GGTGGGAAGAACGACGAGAGGGAAGACAGCG GGAAGAGTAGGTCGCAGTGTC	FAM	

Table 2. Table of antibodies used in the thesis.

Primary antibody	**Animal origin**	**Source**
anti-FITC monoclonal IgG2a	Mouse	GenWay Biotech
isotype monoclonal IgG2a	Mouse	GenWay Biotech
Mouse serum	Mouse	Purified from BALB/c mice
Mouse plasma	Mouse	Purified from BALB/c mice
Human intraveneous immunoglobulin (hIVIG)	Human	Talecris Biotherapeutics
M86 anti-Gal polyclonal IgG	Mouse	Dr. Uri Galili (University of Massachusetts Medical School, Worcester, MA)
M86 anti-Gal polyclonal IgM	Mouse	Dr. Uri Galili (University of Massachusetts Medical School, Worcester, MA)

Secondary antibody	**Animal origin**	**Species detected**	**Source**
Alexa Fluor 647 IgG	Goat	Mouse	Life Technologies
Alexa Fluor 647 IgM	Goat	Mouse	Life Technologies
C3/C3b/iC3b monoclonal	Rat	Mouse/human	Cedarlane

FIGURES

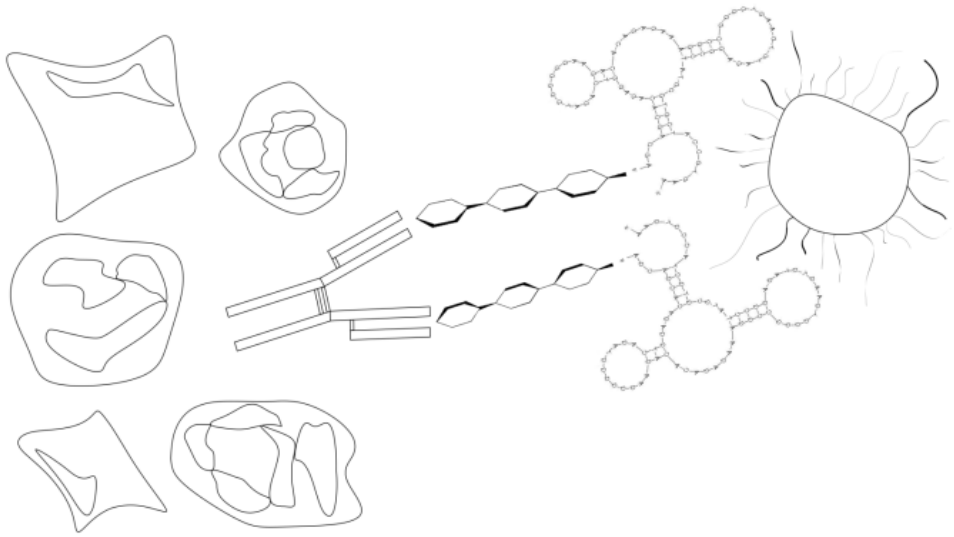

Figure 1. A schematic model for the mode-of-action (MOA) of alphamer-mediated therapy. From right to left, target bacterium is bound by target-specific alphamers, which are aptamers conjugated with the alpha-Gal epitope. The alpha-Gal epitope is an immunostimulatory in its effect of recruiting anti-alpha-Gal antibodies, which are preexisting in abundance in humans. Recruited anti-alpha-Gal antibodies, especially IgG, can direct neutrophils and macrophages – which many pathogens have evolved to evade – and lead to clearance of target pathogens via phagocytosis and complement activation.

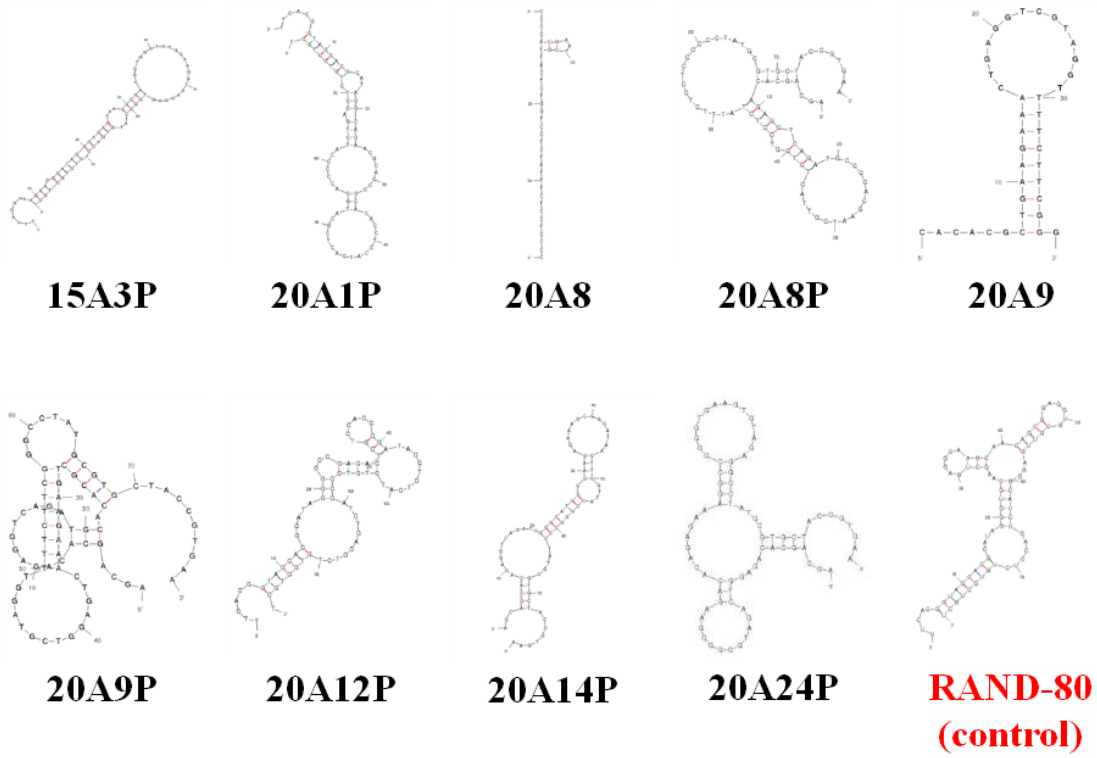

Figure 2. Secondary structure models of the nine DNA aptamers described in Hamula *et al.* (13) and a control DNA aptamer RAND-80 (80-nt). The secondary structure models were predicted by the Mfold web server, which generates a model of single stranded nucleic acids by determining the lowest free energy.

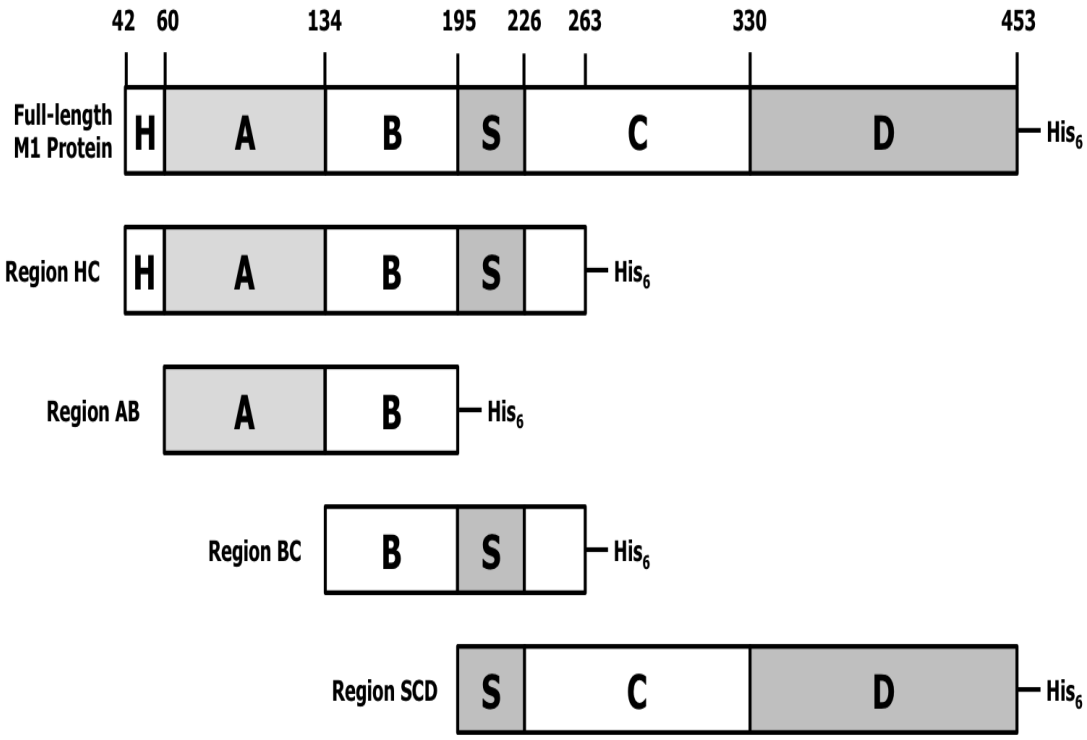

Figure 3. A schematic of GAS M1 protein showing the different regions. GAS M1 protein and the protein's truncated constructs were received from Dr. Partho Ghosh (Department of Chemistry and Biochemistry, University of California San Diego, La Jolla, CA). The A and B regions are hypervariable and variable, respectively, while the C and D regions are generally conserved in GAS strains.

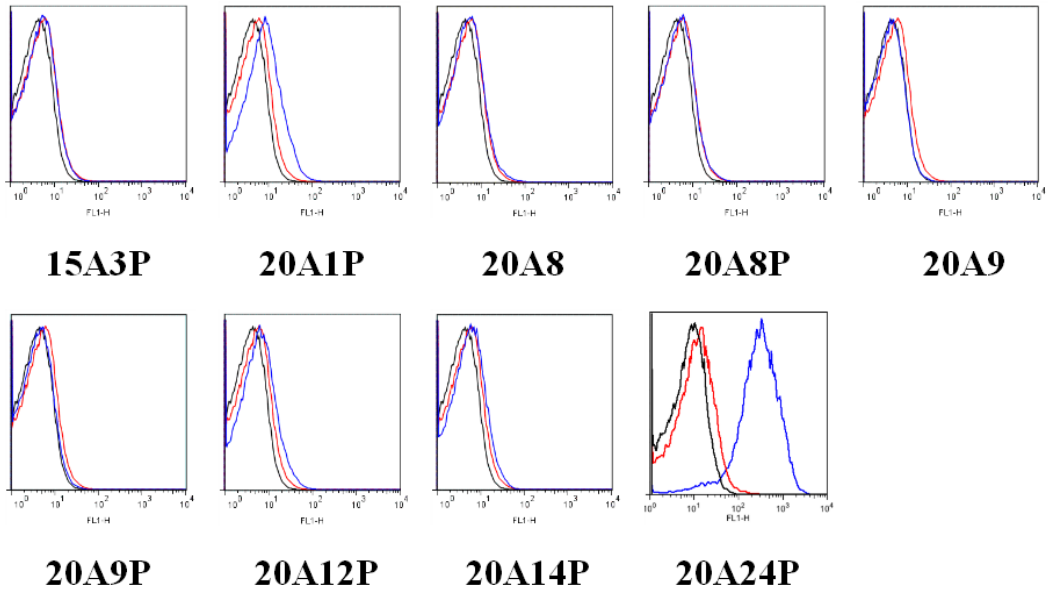

Figure 4. Binding of nine FAM-labeled DNA aptamers described in Hamula *et al.* (13). Live, stationary phase GAS M1 5448 cells were incubated with 5'-FAM-labeled aptamer (blue line), 5'-FAM-labeled RAND-80 control aptamer (red line), or aptamer vehicle (black line) for 30 – 45 minutes in normal atmosphere at 37°C. GAS cells were washed and the fluorescence levels of 20,000 gated particles per sample were measured at FL-1 channel. Fluorescence shift with 20A24P aptamer-treated cells compared to that of RAND-80 control aptamer- and aptamer vehicle-treated cells indicates binding of 20A24P to GAS cells. Aptamer 20A24P was prioritized as the lead candidate aptamer for this proof-of-concept (POC) project.

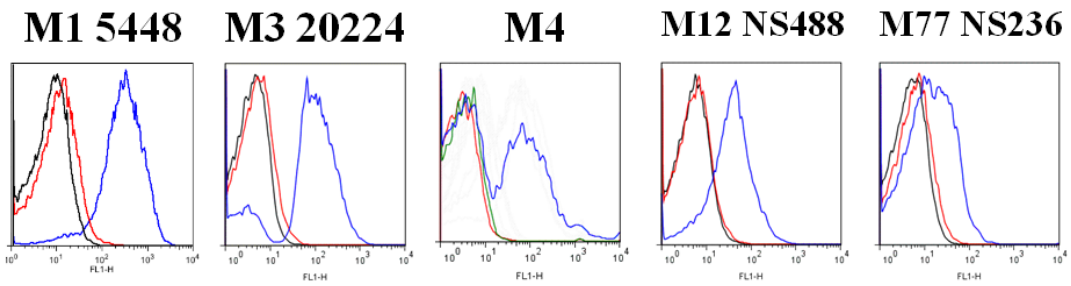

Legend – Blue: GAS aptamer; Red: Control aptamer; **Black**: Aptamer vehicle

Figure 5. Broad spectrum binding 20A24P aptamer to GAS bacteria of multiple serotypes. Live, stationary phase GAS bacteria of multiple serotypes were incubated with 5'-FAM-20A24P, 5'-FAM-RAND-80, or aptamer vehicle, washed, and subjected to FL-1 fluorescence channel. Binding of 20A24P aptamer to multiple serotypes of GAS confirms the broad spectrum binding as described in Hamula *et al.* publication (13).

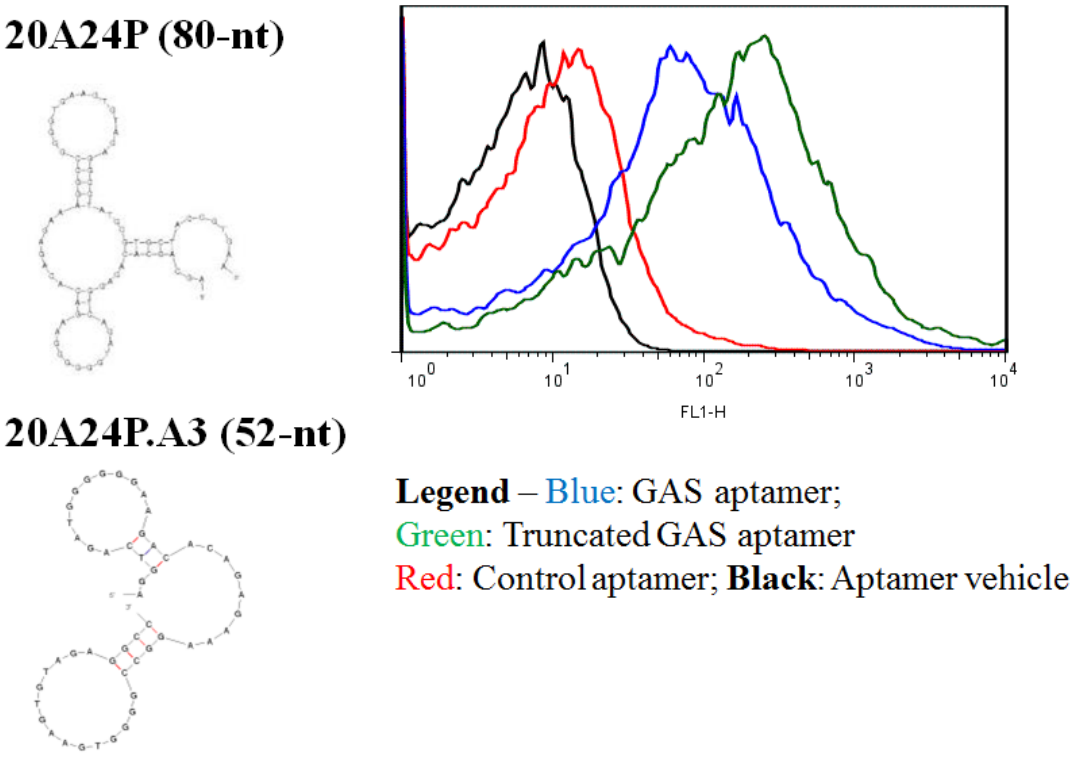

Figure 6. Truncation enhances the binding of 20A24P aptamer to GAS M1 5448 bacteria. Secondary structures of 20A24P aptamer (left, top) and its truncated variant A3 (20A24P.A3; left, bottom). Live, stationary phase GAS M1 5448 bacteria were incubated with 5'-FAM-20A24P full-length aptamer, 5'-FAM-20A24P.A3 truncated aptamer, 5'-FAM-RAND-80 control aptamer, or aptamer vehicle, washed, and subjected to FL-1 fluorescence channel (right). The A3 truncated variant showed greater fluorescence shift (green) than the full-length aptamer (blue), indicating enhanced binding to GAS M1 5448 bacteria.

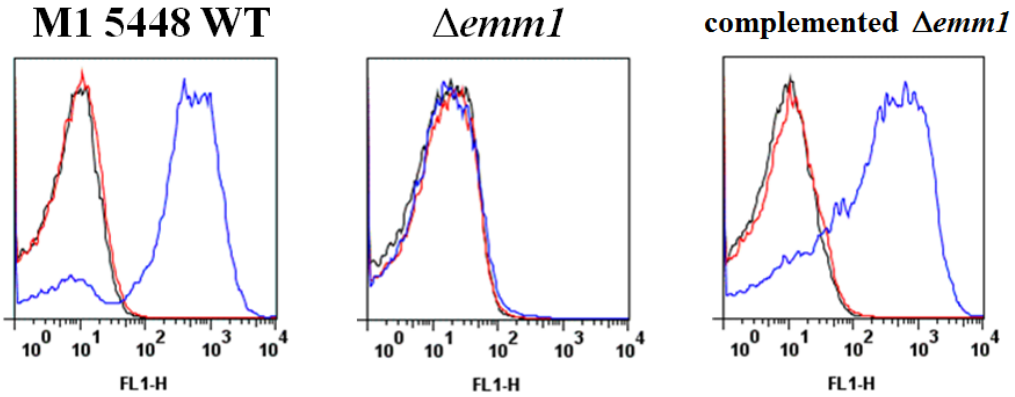

Legend – Blue: GAS aptamer; Red: Control aptamer; **Black**: Aptamer vehicle

Figure 7. Loss-gain of 20A24P aptamer binding with GAS *emm1* gene. Live, stationary phase GAS M1 5448 wild-type, GAS M1 5448 Δ*emm1*, and GAS M1 5448 Δ*emm1* complemented with *emm1* were incubated with 5'-FAM-20A24P, 5'-FAM-RAND-80, or aptamer vehicle, washed, and subjected to FL-1 fluorescence channel. 20A24P aptamer did not bind to the *emm1* mutant strain, but bound to the wild-type and the complemented *emm1* mutant strain. M1 protein is the product of *emm1* gene and the target antigen of 20A24P aptamer was proposed as either the M1 protein or an antigen that requires the expression of *emm1* gene.

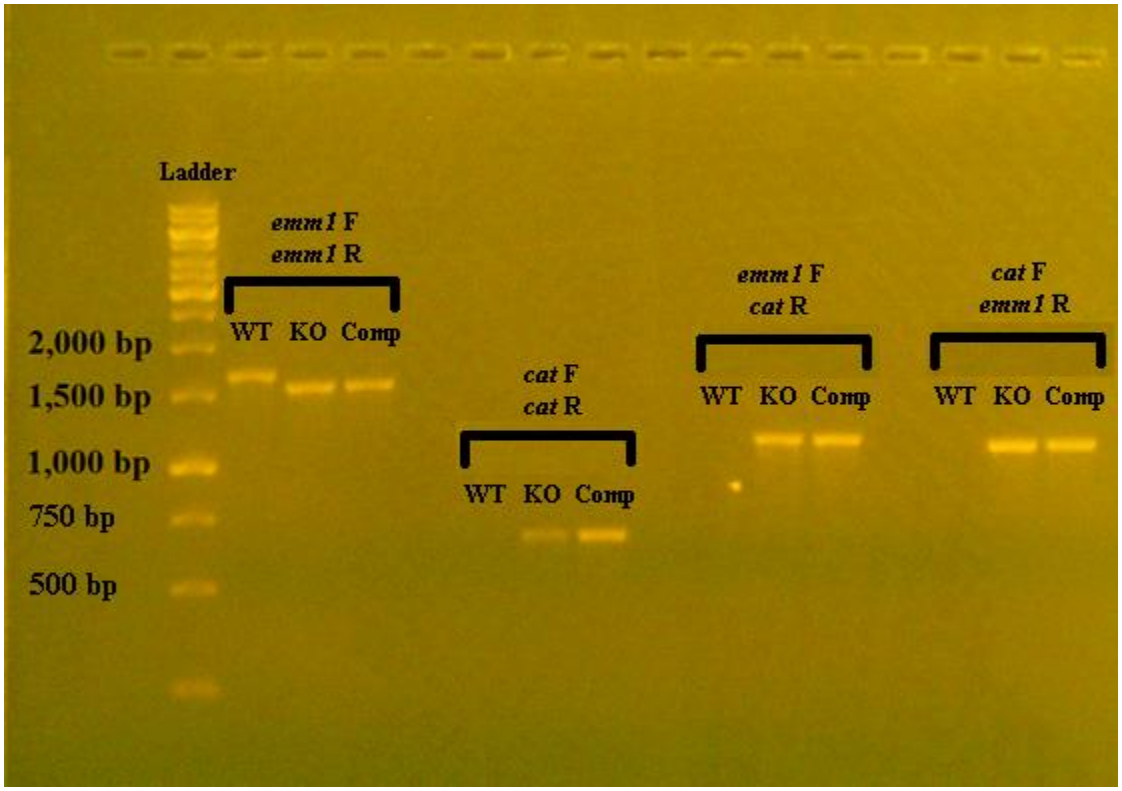

Figure 8. A gel electrophoresis confirmation of *emm1* mutagenesis. DNA samples of GAS M1 5448 wild-type ("WT"), GAS M1 5448 Δ*emm1* ("KO"), and GAS M1 5448 Δ*emm1* pDCerm-*emm1* ("comp") extracted using Bactozol Bacterial DNA Isolation Kit and used in gel electrophoresis to(12 confirm that the mutant strains were indeed deficient for the *emm1* gene as described in Lauth *et al.* (15). In the first primer set (*emm1* forward and *emm1* reverse), the band for WT strain (~1,600 bp) is slightly larger than those of mutant and complemented mutant strains, which were described to have been partially deleted. In the second primer set (*cat* forward and *cat* reverse), two bands of approximately 650 bp appeared only for the mutant and the complemented mutant strains, which correspond to the *cat* amplicon used in *E. coli* Top10 cells (15). The third and the fourth primer sets show bands for the mutant and the complemented mutant strains, confirming that the *cat* gene is within the *emm1* gene, which has been interrupted and partially deleted.

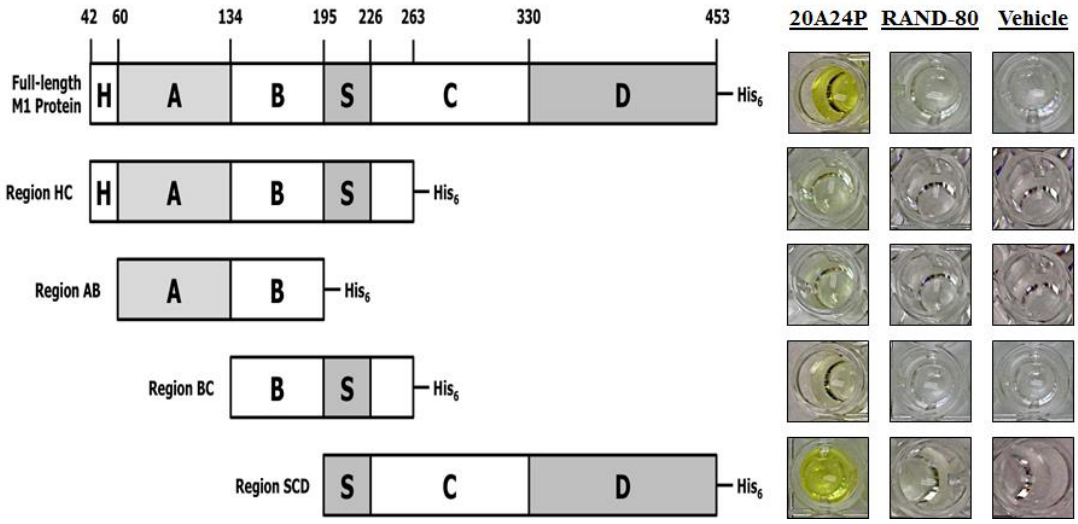

Figure 9. A schematic of GAS M1 protein and binding of biotinylated 20A24P aptamer to M1 protein. In a colorimetric ELISA, wells were coated with the full-length M1 protein and its truncated variants, washed, and incubated with biotinylated 20A24P-3' BioTeg 3', biotinylated RAND-80-3' BioTEG, or aptamer vehicle. Wells were washed and aptamer binding was detected by horseradish peroxide (HRP)-conjugated streptavidin, which developed yellow color after incubating with 3,3'-5,5'-Tetramethylbenzidine (TMB) substrate. Biotinylated aptamer 20A24P bound strongly to the full-length M1 protein and the highly conserved region SCD, confirming an earlier suggestion that the binding target of 20A24P aptamer is the M1 protein.

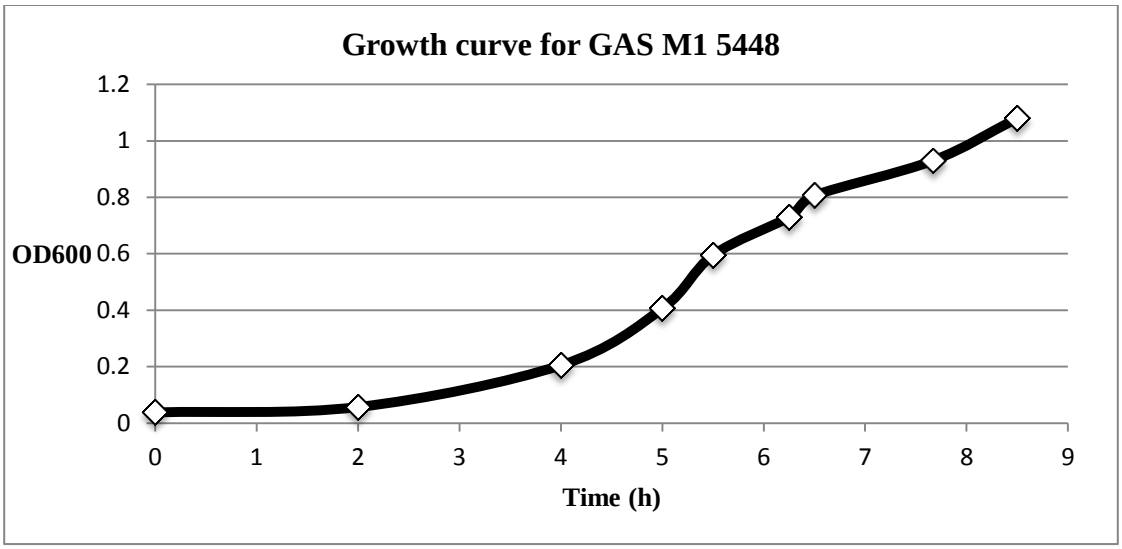

Figure 10. Growth curve of GAS M1 5448 bacteria. Overnight culture of GAS M1 5448 was diluted to optical density at 600 nm (OD_{600}) near 0 (OD_{600} = 0.038) and incubated for 8.5 hours with intermittent OD_{600} reading. OD_{600} values of 0.3, 0.5, 0.8, and ≥0.9 were considered early-exponential, mid-exponential, late-exponential, and stationary phase, respectively.

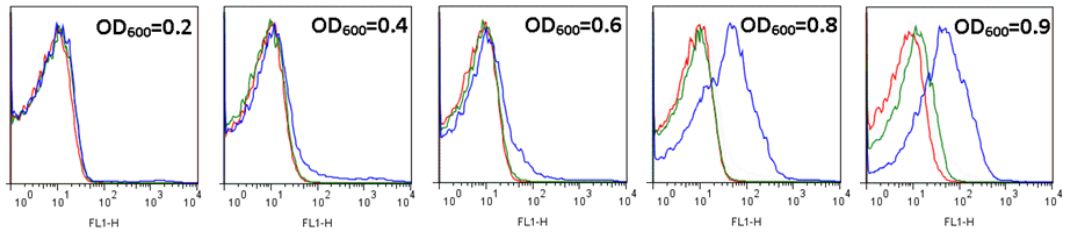

Legend – Blue: GAS aptamer; Red: Control aptamer; **Black**: Aptamer vehicle

Figure 11. Growth phase-dependent binding of 5'-FAM-20A24P 3' to GAS M1 5448 bacteria. Overnight culture of GAS M1 5448 bacteria was diluted to OD_{600} near 0, incubated and harvested at different optical densities, and placed on ice until the last OD_{600} sample was collected. GAS bacteria of different optical densities were incubated with 5'-FAM-20A24P, 5'-FAM-RAND-80, or aptamer vehicle, washed, and subjected to fluorescence FL-1 channel. The 20A24P aptamer selectively binds to GAS bacteria in late-exponential (OD_{600}=0.8) and stationary (OD_{600}=0.9) phases, but not to GAS in earlier growth phases.

Figure 12A

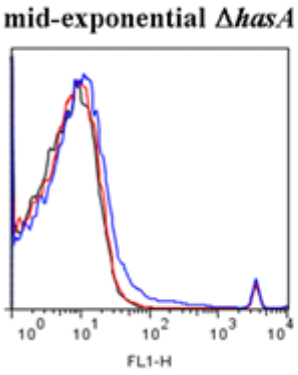

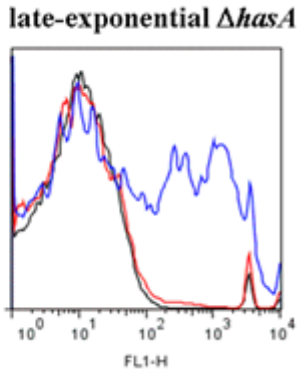

Figure 12B

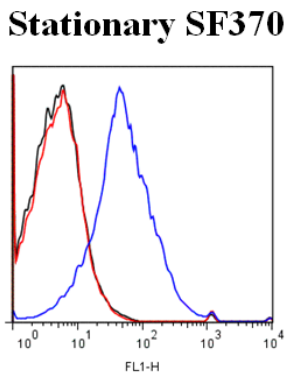

Figure 12C

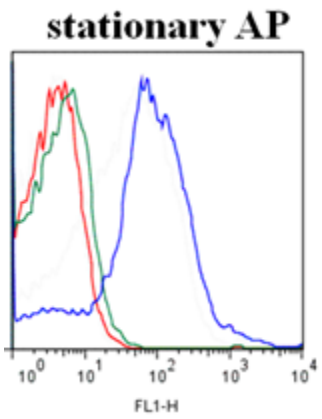

Figure 12D

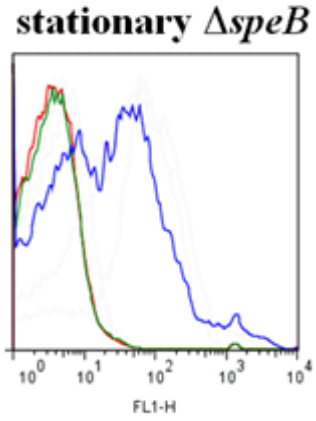

Figure 12E

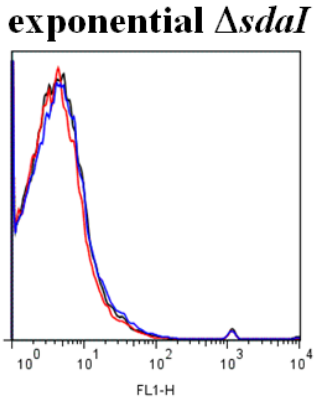

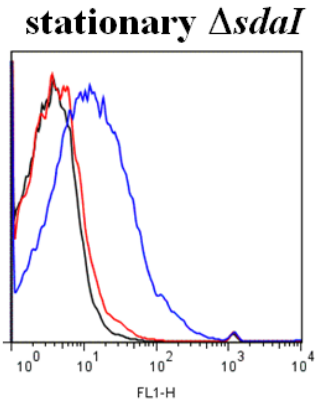

Legend –
Blue: GAS aptamer;
Red: Control aptamer;
Black: Aptamer vehicle

Figure 12. Binding of 5'-FAM-20A24P to GAS M1 5448 mutant strains and GAS M1 SF370 bacteria. GAS bacteria were incubated with 5'-FAM-20A24P, 5'-FAM-RAND-80, or aptamer vehicle, washed, and subjected to fluorescence FL-1 channel. (A, B, and C) 5'-FAM-20A24P did not bind to live, mid-exponential phase GAS M1 5448 Δ*hasA* cells, but did bind to stationary phase bacteria. The aptamer showed

significant binding to live, late-exponential phase GAS M1 SF370 cells, a strain which produces less hyaluronic acid (HA) capsule, as well as GAS M1 5448 animal-passage (AP) cells, a strain which produces more HA capsule. As the binding of 20A24P aptamer was not affected by reduced or increased HA capsule, it was determined that the HA capsule does not affect 20A24P aptamer binding to the M1 protein. (D) 20A24P aptamer bound to live, stationary phase GAS M1 5448 Δ*speB* cells, a strain which lacks the SpeB cysteine protease, and showed that the binding of 20A24P to the M1 protein is not affected by SpeB protease processing. (E) Lastly, 20A24P aptamer bound to stationary-phase GAS M1 5448 Δ*sda1* cells, a strain which lacks the Sda1 DNase, and showed that the binding of 20A24P is not affected by Sda1 DNase activity.

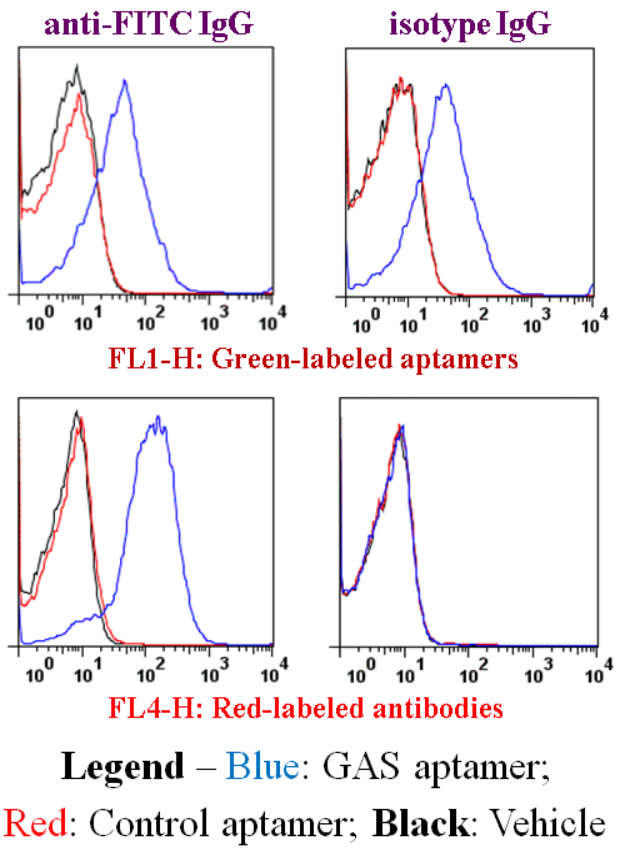

Figure 13. Binding of 5'-FAM-20A24P 3' to GAS M1 5448 and recognition of bound aptamers by anti-FITC IgG. Live, stationary phase GAS M1 5448 bacteria were incubated firstly with 5'-FAM-20A24P aptamer, 5'-FAM-RAND-80 control aptamer, or aptamer vehicle, secondly with anti-FITC IgG_{2a} mAb primary antibody (left), isotype IgG_{2a} mAb primary antibody (right), or antibody vehicle, and thirdly with Alexa Fluor 647 anti-mouse IgG secondary antibody (bottom) or antibody vehicle. Samples were washed between each incubation. 20A24P aptamer bound to GAS M1 5488 bacteria as observed at FL-1 channel, and anti-FITC IgG antibody bound to the GAS-bound aptamer as observed at FL-4 channel.

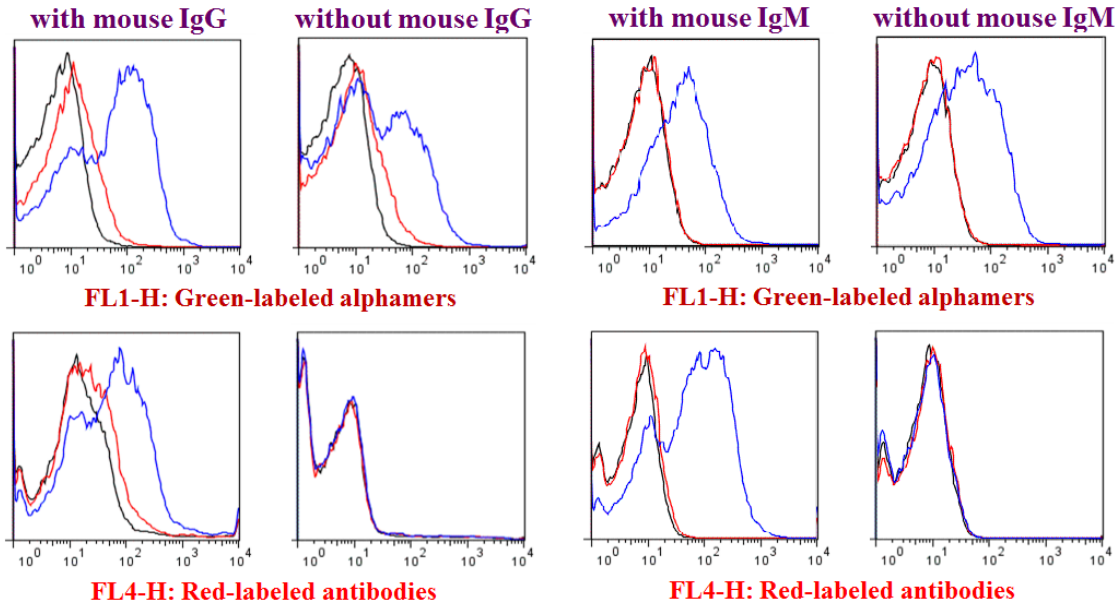

Figure 14. Binding of 5'-alpha-Gal-20A24P-FAM-3' to GAS M1 5448 bacteria and recognition of bound alphamer by M86 anti-alpha-Gal antibody IgG and IgM. Live, stationary phase GAS M1 5448 bacteria were incubated firstly with 5'-alpha-Gal, 3'-FAM alphamer α20A24P or 5'-alpha-Gal, 3'-FAM control alphamer αRAND-80, or alphamer vehicle (top four histograms); secondly with M86 polyclonal IgG (left four histograms), M86 IgM (right four histograms) or antibody vehicle; and thirdly with detection antibody Alexa Fluor 647 anti-mouse IgG, anti-mouse IgM, or antibody vehicle (bottom four histograms). Samples were washed between each incubation. α20A24P bound to GAS M1 5448 bacteria as observed at FL-1 channel, and anti-alpha-Gal IgG or IgM bound to the GAS-bound alphamer as observed at FL-4 channel.

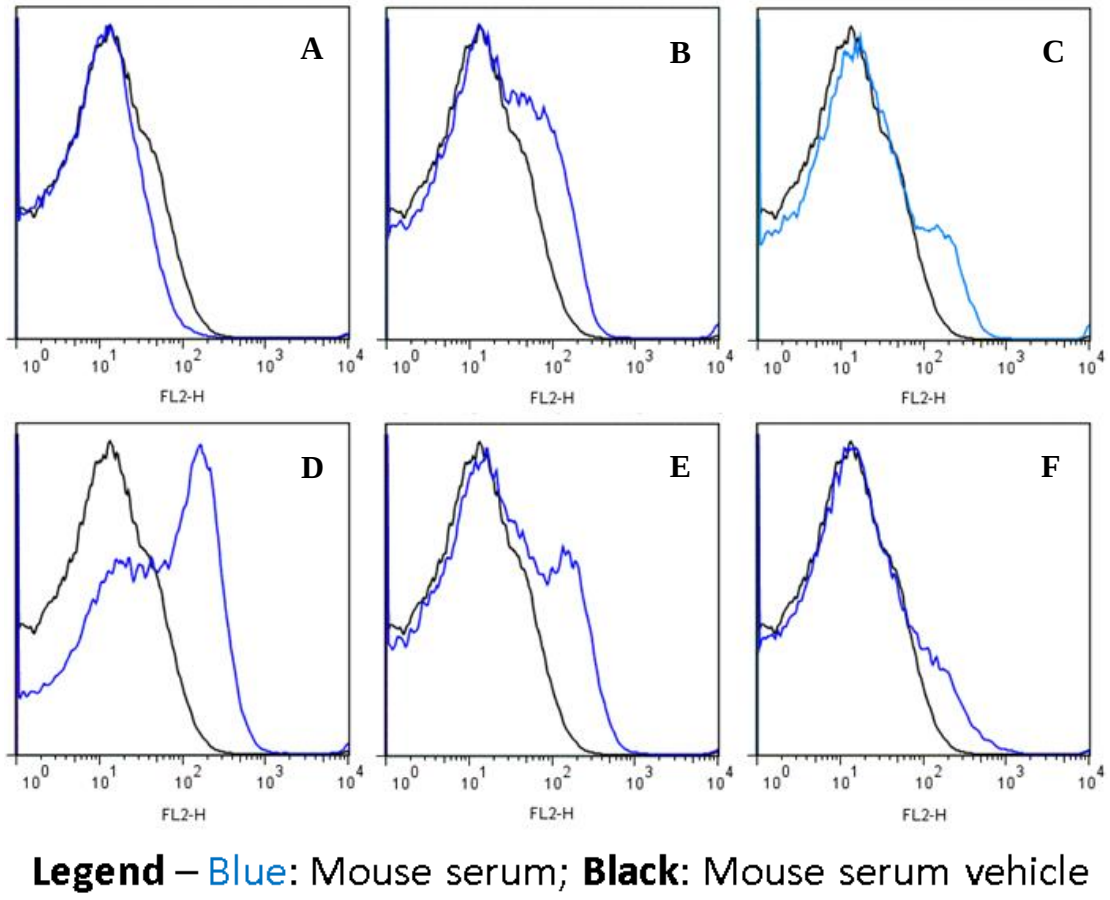

Figure 15. Deposition of complement by mouse serum on GAS M1 5448 cells. Live, stationary phase GAS M1 5448 bacteria were incubated firstly with 0.5% (A) to 3% (F) mouse serum or serum vehicle; secondly with PE-labeled rat anti-mouse/human C3/C3b/iC3b antibody; and subjected to fluorescence FL-2 channel. Samples were washed between each incubation. A clear, increasing fluorescence shift trend with increasing dose of mouse serum was not observed and the baseline level of complement deposition was not established.

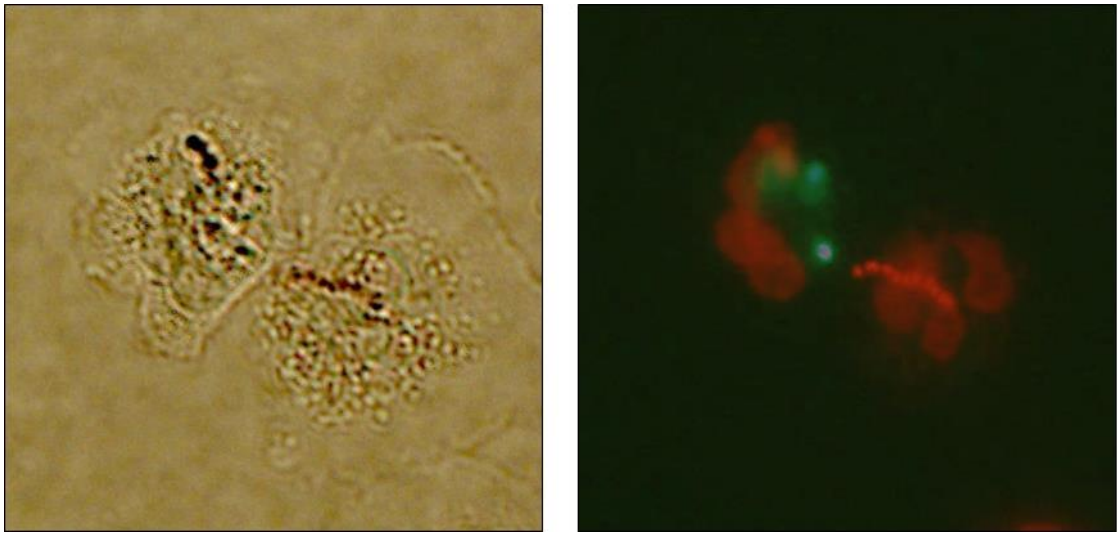

Figure 16. Microscope views of intracellular and extracellular fluorescent GAS M1 5448 cells. Calcein-AM-loaded GAS M1 5448 bacteria appeared green fluorescence after overnight growth. Live, late exponential phase GAS bacteria were washed, incubated firstly with 5'-alpha-Gal, 3'-FAM alphamer α20A24P or 5'-alpha-Gal, 3'-FAM control alphamer αRAND-80, or alphamer vehicle; secondly with M86 anti-alpha-Gal IgG, human intravenous immunoglobulin (hIVIG), or antibody vehicle; and thirdly with purified human neutrophils (hPMNs) or neutrophil vehicle. Samples were washed between each incubation, and after the last incubation, they were diluted 1:1 in 10 mg/mL ethidium bromide and viewed with light (left) and fluorescence channels (right). GAS bacteria phagocytosed by neutrophils (intracellular) were green and those outside of neutrophils were red.

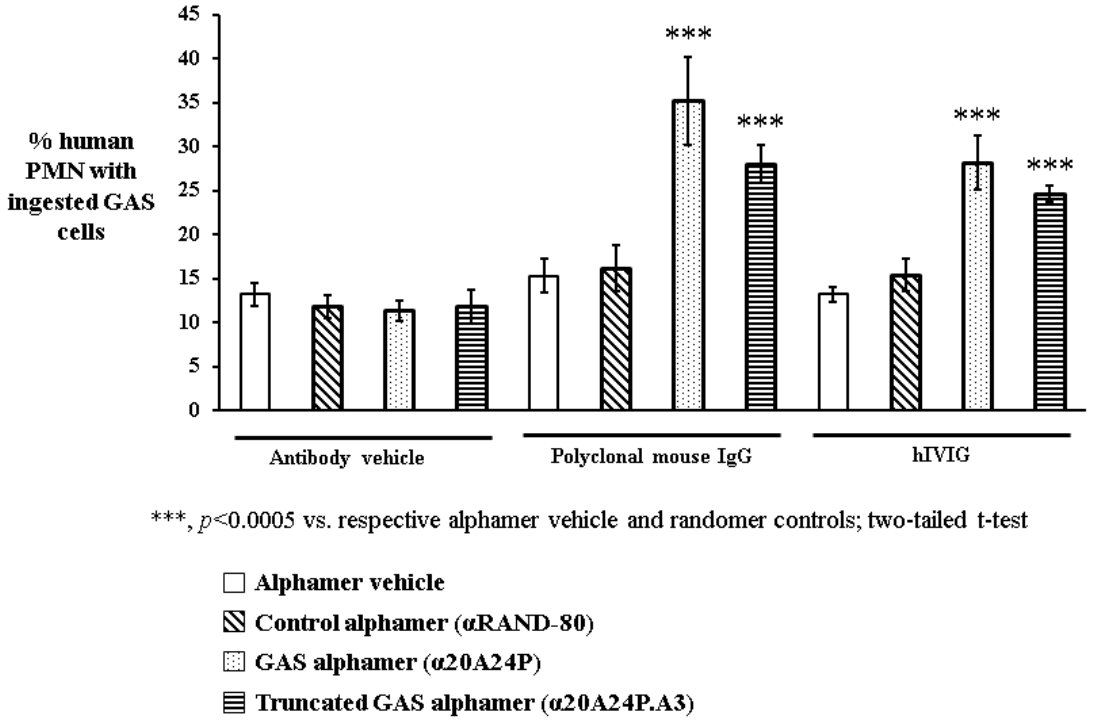

Figure 17. Increased uptake of GAS M1 5448 bacteria by hPMNs with α20A24P treatment and anti-alpha-Gal antibody incubation. Live, late exponential phase GAS M1 5448 bacteria loaded with calcein-AM during overnight incubation were incubated firstly with 5'-alpha-Gal, 3'-FAM alphamers α20A24P, truncated non-FAM labeled 5'-alpha-Gal GAS alphamer α20A24P.A3 or 5'-alpha-Gal, 3'-FAM control alphamer αRAND-80, or alphamer vehicle; secondly with M86 anti-alpha-Gal IgG, hIVIG, or antibody vehicle; and thirdly with hPMNs or neutrophil vehicle. Samples were washed between each incubation, and after the last incubation, they were diluted in 1:1 10 mg/mL ethidium bromide. With a fluorescence microscope, 100 to 200 hPMNs per sample were observed for phagocytosis of GAS bacteria. There was a significant increase in uptake of GAS cells by hPMNs when treated with α20A24P and in the presence of anti-alpha-Gal antibody (polyclonal M86 IgG or hIVIG).

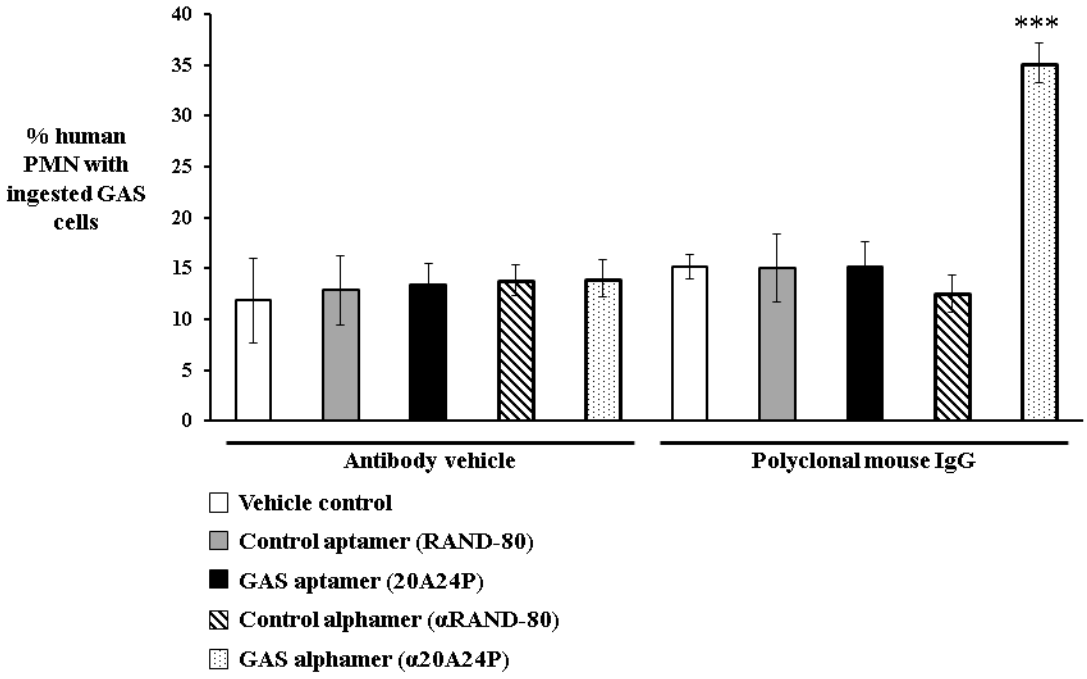

Figure 18. Increased phagocytic function of hPMNs is dependent on the alpha-Gal epitope of α20A24P. Microscope samples were prepared as described in **Figure 18**, except GAS M1 5448 cells were incubated with non-alpha-Gal conjugated 3'-FAM labeled GAS aptamer 20A24P or 3'-FAM RAND-80 alongside alphamers to show that in the presence of anti-alpha-Gal antibody (M86 IgG), only α20A24P treatment leads to the increased uptake of GAS by hPMNs, and the effect was dependent on the alpha-Gal epitope.

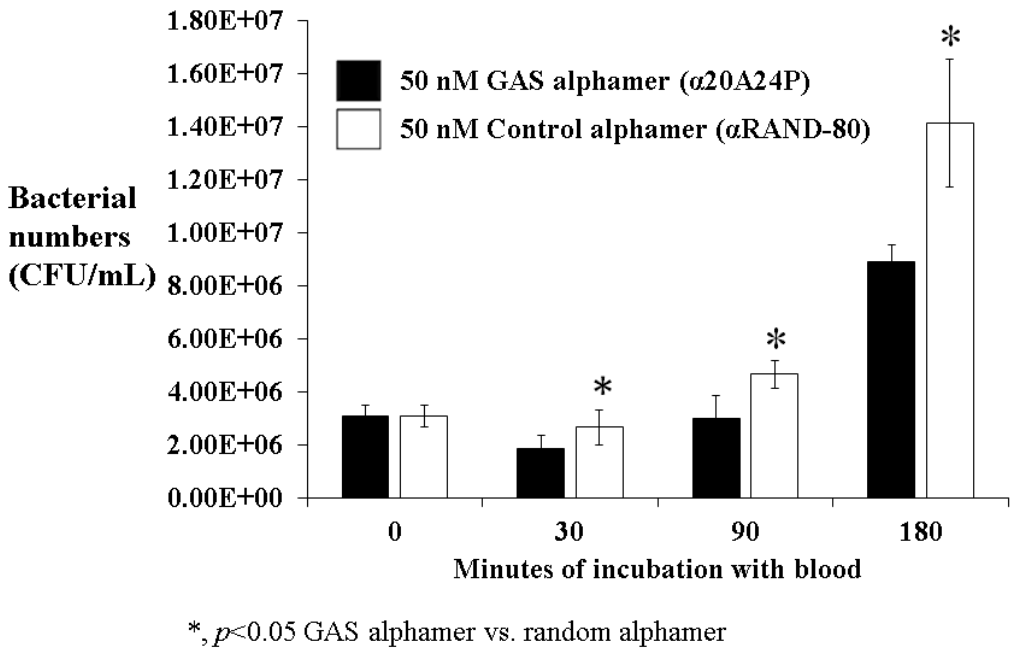

Figure 19. Preliminary whole blood killing assay (WBKA) data showing impairment of the outgrowth of GAS M1 5448 cells by α20A24P in human whole blood. Live, late exponential phase GAS M1 5448 bacteria were incubated firstly with 5'-alpha-Gal-20A24P alphamer, 5'-alpha-Gal-RAND-80 control alphamer, or control alphamer; secondly with human whole blood; and plated at different time points after incubating with whole blood. CFU were determined after overnight incubation. α20A24P treatment did not lead to direct killing of GAS M1 5448, but rather but rather significantly impaired the outgrowth of the hypervirulent strain.

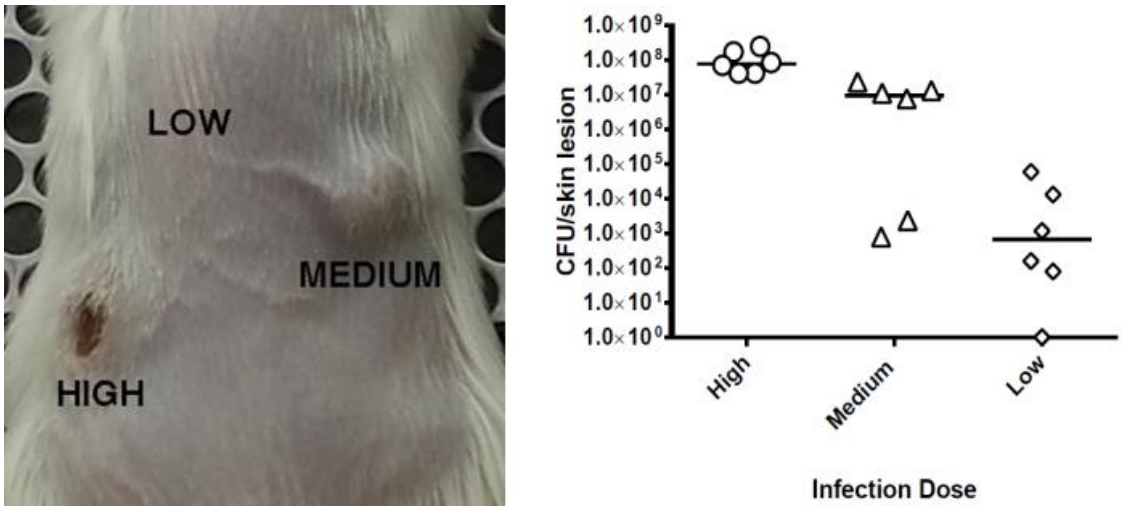

Figure 20. Dose-dependent lesion formation and surviving GAS colony forming units (CFU)/mL. (left) Dose-dependent formation of lesion for GAS skin infection model, where BALB/c $GT^{-/-}$ mice mutant deficient in the production of the alpha-Gal epitope (8) were injected subcutaneously with low inoculum ($1x10^7$ CFU/mL), medium inoculum ($1x10^8$ CFU/mL), and high inoculum ($1x10^9$ CFU/mL) of GAS M1 5448 bacteria. (right) Skin samples containing GAS cells were harvested 96 hours after injection, homogenized, plated, and CFU/mL for each inoculum was determined after overnight incubation. Approximately $1x10^3$ CFU/mL, $1x10^7$ CFU/mL, and $1x10^8$ CFU/mL GAS bacteria were recovered from low ($1x10^7$ CFU/mL), medium ($1x10^8$ CFU/mL), and high ($1x10^9$ CFU/mL) inocula injection, which is consistent with no skin perturbation, abscess formation, and lesion formation at low, medium, and high inocula infection sites.

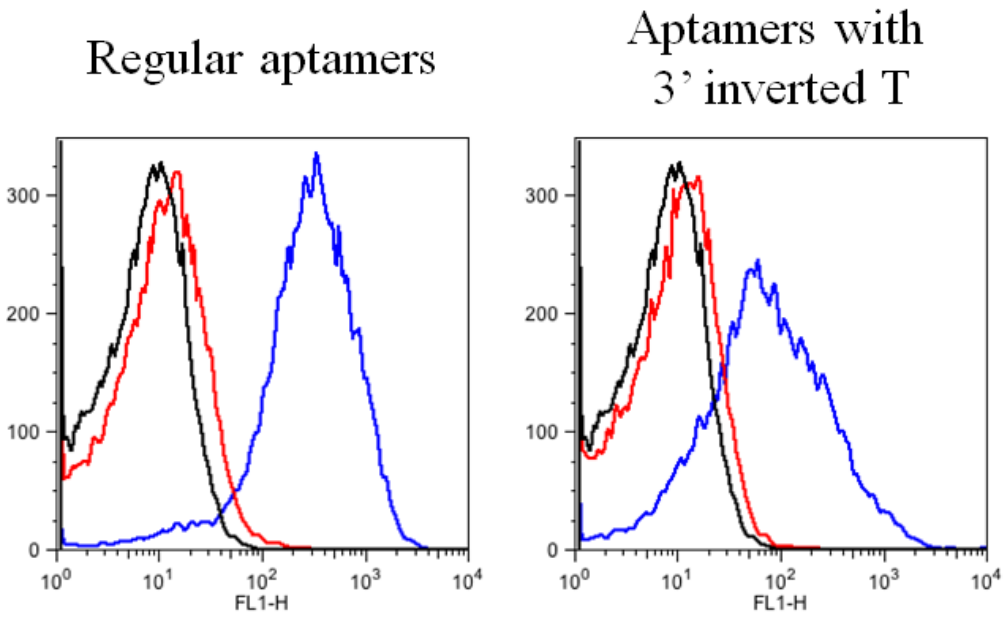

Figure 21. Binding of 5'-FAM-20A24P-dT-3' to GAS M1 5448. Live, stationary phase GAS M1 5448 were incubated with FAM-labeled, inverted thymidine (dT)-conjugated aptamers (5'-FAM-20A24P-dT-3', 5'-FAM-20A24P-dT-3', or aptamer vehicle) and subjected to fluorescence FL-1 channel. Conjugation of 20A24P at 3' end with dT did not alter the binding pattern of 20A24P aptamer, and it will increase its nuclease resistance against 3' exonucleases by creating a 3'-3' linkage.

REFERENCES

1. **Kuehnert MJ, Kruszon-Moran D, Hill HA, McQuillan G, McAllister SK, Fosheim G, McDougal LK, Chaitram J, Jensen B, Fridkin SK, Killgore G, Tenover FC.** 2006. Prevalence of Staphylococcus aureus nasal colonization in the United States, 2001-2002. J. Infect. Dis. **193**(2):172-9.

2. **Infectious Diseases Society of America (IDSA), Spellberg B, Blaser M, Guidos RJ, Boucher HW, Bradley JS, Eisenstein BI, Gerding D, Lynfield R, Reller LB, Rex J, Schwartz D, Septimus E, Tenover FC, Gilbert DN.** 2011. Combating antimicrobial resistance: policy recommendations to save lives. Clin. Infect. Dis. **52** Suppl 5:S397-428.

3. **Klevens RM, Morrison MA, Nadle J, Petit S, Gershman K, Ray S, Harrison LH, Lynfield R, Dumyati G, Townes JM, Craig AS, Zell ER, Fosheim GE, McDougal LK, Carey RB, Fridkin SK; Active Bacterial Core surveillance (ABCs) MRSA Investigators.** 2007. Invasive methicillin-resistant Staphylococcus aureus infections in the United States. JAMA. **298**(15):1763-71.

4. **Klevens RM, Edwards JR, Richards CL Jr., et al.** 2002. Estimating health care-associated infections and deaths in U.S. hospitals, 2002. Public Health Rep. **122**(2):160-6.

5. **Centers for Disease Control and Prevention.** 2013. Antibiotic resistance threats in the United States, 2013.

6. **Jenkins SG, Brown SD, Farrell DJ.** 2008. Trends in antibacterial resistance among Streptococcus pneumoniae isolated in the USA: update from PROTEKT US Years 1-4. Ann. Clin. Microbiol. Antimicrob. **7**:1.

7. **Spellberg B, Guidos R, Gilbert D, Bradley J, Boucher HW, Scheld WM, Bartlett JG, Edwards J Jr; Infectious Diseases Society of America.** 2008. The epidemic of antibiotic-resistant infections: a call to action for the medical community from the Infectious Diseases Society of America.

8. **Galili U.** 2013. Discovery of the natural anti-alpha-Gal antibody and its past and future relevance to medicine. Xenotransplantation. doi: 10.1111/xen.12034.

9. **Galili U, Mandrell RE, Hamadeh RM, Shohet SB, Griffiss JM.** 1988. Interaction between human natural anti-alpha-Galactosyl immunoglobulin G and bacteria of the human flora. Infect. Immun. **56**(7):1730-7.

10. **Galili U, Anaraki F, Thall A, Hill-Black C, Radic M.** 1993. One percent of human circulating B lymphocytes are capable of producing the natural anti-alpha-Gal antibody. Blood. **82**(8):2485-93.

11. **Ohuchi S.** 2012. Cell-SELEX Technology. Biores. Open Access. **1**(6):265-72.

12. **Keefe AD, Pai S, Ellington A.** 2010. Aptamers as therapeutics. Nat. Rev. Drug Discov. **9**(7):537-50.

13. **Hamula CL, Le XC, Li XF.** 2011. DNA aptamers binding to multiple prevalent M-types of Streptococcus pyogenes. Anal. Chem. **83**(10):3640-7.

14. **Chatellier S, Ihendyane N, Kansal RG, Khambaty F, Basma H, Norrby-Teglund A, Low DE, McGeer A, Kotb M.** 2000. Genetic relatedness and superantigen expression in group A streptococcus serotype M1 isolates from patients with severe and nonsevere invasive diseases. Infect. Immun. **68**(6):3523-34.

15. **Lauth X, von Köckritz-Blickwede M, McNamara CW, Myskowski S, Zinkernagel AS, Beall B, Ghosh P, Gallo RL, Nizet V.** 2009. M1 protein allows Group A streptococcal survival in phagocyte extracellular traps through cathelicidin inhibition. J. Innate. Immun. **1**:202–214.

16. **Hollands A, Pence MA, Timmer AM, Osvath SR, Turnbull L, Whitchurch CB, Walker MJ, Nizet V.** 2010. Genetic switch to hypervirulence reduces colonization phenotypes of the globally disseminated group A streptococcus M1T1 clone. J. Infect. Dis. **202**(1):11-9.

17. **Buchanan JT, Simpson AJ, Aziz RK, Liu GY, Kristian SA, Kotb M, Feramisco J, Nizet V.** 2006. DNase expression allows the pathogen group A Streptococcus to escape killing in neutrophil extracellular traps. Curr. Biol. **16**(4):396-400.

18. **Kansal RG, Nizet V, Jeng A, Chuang WJ, Kotb M.** 2003. Selective modulation of superantigen-induced responses by streptococcal cysteine protease. J. Infect. Dis. **187**(3):398-407.

19. **McKay FC, McArthur JD, Sanderson-Smith ML, Gardam S, Currie BJ, Sriprakash KS, Fagan PK, Towers RJ, Batzloff MR, Chhatwal GS, Ranson M, Walker MJ.** 2004. Plasminogen binding by group A streptococcal isolates from a region of hyperendemicity for streptococcal skin infection and a high incidence of invasive infection. Infect. Immun. **72**(1):364-70.

20. **Zuker M.** 2003. Mfold web server for nucleic acid folding and hybridization prediction. Nucleic Acids Res. **31**(13):3406-15.

21. **Facklam R, Beall B, Efstratiou A, Fischetti V, Johnson D, Kaplan E, Kriz P, Lovgren M, Martin D, Schwartz B, Totolian A, Bessen D, Hollingshead S, Rubin F, Scott J, Tyrrell G.** 1999. emm typing and validation of provisional M types for group A streptococci. Emerg. Infect. Dis. **5**(2):247-53.

22. **Tearle RG, Tange MJ, Zannettino ZL, Katerelos M, Shinkel TA, Van Denderen BJ, Lonie AJ, Lyons I, Nottle MB, Cox T, Becker C, Peura AM, Wigley PL, Crawford RJ, Robins AJ, Pearse MJ, d'Apice AJ.** 1996. The alpha-1,3-galactosyltransferase knockout mouse. Implications for xenotransplantation. Transplantation. **61**(1):13-9.

23. **Jayasena SD.** 1999. Aptamers: an emerging class of molecules that rival antibodies in diagnostics. Clin. Chem. **45**(9):1628-50.

24. **Unnikrishnan M, Cohen J, Sriskandan S.** 1999. Growth-phase-dependent expression of virulence factors in an M1T1 clinical isolate of Streptococcus pyogenes. Infect. Immun. **67**(10):5495-9.

25. **Maamary PG, Ben Zakour NL, Cole JN, Hollands A, Aziz RK, Barnett TC, Cork AJ, Henningham A, Sanderson-Smith M, McArthur JD, Venturini C, Gillen CM, Kirk JK, Johnson DR, Taylor WL, Kaplan EL, Kotb M, Nizet V, Beatson SA, Walker MJ.** 2012. Tracing the evolutionary history of the pandemic group A streptococcal M1T1 clone. FASEB J. **26**(11):4675-84.

26. **Raeder R, Woischnik M, Podbielski A, Boyle MD.** 1998. A secreted streptococcal cysteine protease can cleave a surface-expressed M1 protein and alter the immunoglobulin binding properties. Res. Microbiol. **149**(8):539-48.

27. **Kaur H, Yung LY.** 2012. Probing high affinity sequences of DNA aptamer against VEGF165. PLoS One. **7**(2):e31196.

28. **Alkan ML, Beachey EH.** 1978. Excretion of lipoteichoic acid by group A streptococci. Influence of penicillin on excretion and loss of ability to adhere to human oral mucosal cells. J. Clin. Invest. **61**(3):671-7.

29. **Kristian SA, Datta V, Weidenmaier C, Kansal R, Fedtke I, Peschel A, Gallo RL, Nizet V.** 2005. D-alanylation of teichoic acids promotes group a streptococcus antimicrobial peptide resistance, neutrophil survival, and epithelial cell invasion. J. Bacteriol. **187**(19):6719-25.

30. **Berggård K, Johnsson E, Morfeldt E, Persson J, Stålhammar-Carlemalm M, Lindahl G.** 2001. Binding of human C4BP to the hypervariable region of M1 protein: a molecular mechanism of phagocytosis resistance in Streptococcus pyogenes. Mol. Microbiol. **42**(2):539-51.